Recent Progress in the Modeling of High-Temperature Creep and Its Application to Alloy Development

L. Shi and D.O. Northwood

Recent progress in the understanding of high-temperature creep of alloys is discussed in the context of theoretical modeling and its application to alloy development. Emphasis is placed upon those engineering alloys specifically designed for high-temperature applications, such as precipitation and dispersion-strengthened (DS) alloys and metal-matrix composites (MMCs). Currently, these theoretical models use one of two different approaches, (a) a phenomenological approach, which is used in such models as those based on the internal stress concept, and those based on empirical creep equations; and (b) micromechanical models that are based on dislocation mechanisms and the interactions of dislocations with solute atoms, second-phase particles, and other reinforcements such as fibers. All these theoretical models have a common goal, namely, the understanding of high-temperature strengthening mechanisms and the relationship between high-temperature strength and the micromechanical mechanisms during high-temperature plastic deformation of the alloys. These theoretical studies can provide information that is useful in alloy design and processing, such as the selection of alloy chemistry, and the optimization of phase microstructural features (e.g., reinforcement amount, shape, size, and distribution; matrix grain size; and matrix and reinforcement interfaces) by optimization of processing methods.

Keywords

alloy development, creep, dislocations, mechanisms

1. Introduction

CREEP, together with fatigue and fracture, are important from both an economic and an academic point of view. Creep is one of a number of fields where improvements could lead to the possibility of rapid technological advance in terms of a more reliable and safer performance, or the attainment of higher energy efficiency. There is a demonstrated need for the development and improvement of materials for various engineering applications at elevated temperatures, and engineers and scientists worldwide are devoting their time and energy to the study and solution of creep-related matters.

Generally, the creep process is described in terms of a strain-time relationship (both the applied stress and test temperature are kept constant during a creep experiment). Figure 1 is a schematic diagram for a typical creep curve of metals and alloys. These are three stages in strain-time behavior in the creep of metals and alloys. In primary creep stage I, where the strain is increasing with time, the rate is decreasing with time (or in some cases increasing). In secondary stage II, the strain is increasing with time at a constant rate (steady-state creep). In tertiary stage III, the creep is accelerating until fracture (Ref 1-3). For polycrystalline materials, creep rupture is generally associated with void formation and the coalescence of microcracks within grains or at grain boundaries.

Since creep is a slow deformation process, long-term tests must be conducted on selected samples before an improved mechanical design is practically attainable and a component is assembled into an operating machine. For creep studies and research, emphasis has been on the steady-state creep stage, its connection to final fracture, and the behavior when either applied stress is varying or when environmental effects come into play (creep-fatigue interactions and creep-corrosion interactions). Previous studies have shown that the creep performance of an engineering material is determined by both properties of the material and its operating environment (e.g., stress and temperature distributions). Such technical (creep) data can be obtained in a number of ways, such as (a) in a long-term

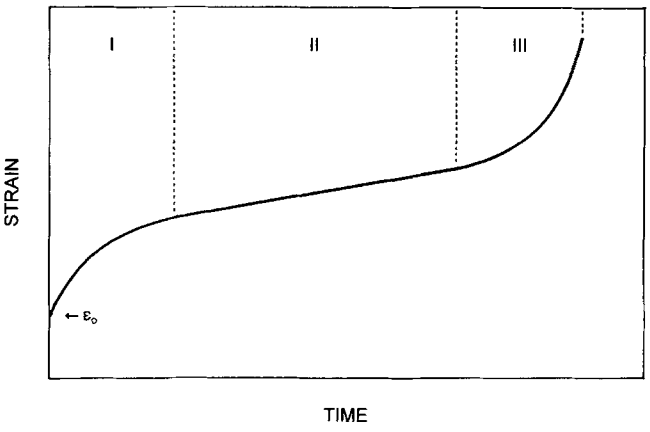

Fig. 1 Typical creep curve (strain-time) showing three stages of creep. ε_0 is the instantaneous elastic strain upon loading. In the course of creep, the creep rate gradually decreases in the primary creep stage I to a steady-state value in steady-state stage II, and then increases in stage III until fracture.

L. Shi, Department of Materials Science and Engineering, University of Virginia, Charlottesville, VA 22901, USA (now at Mechanical Engineering Dept., University of Waterloo, Waterloo, Ontario N2l3G1 Canada): and **D.O. Northwood,** Engineering Materials Group, Mechanical Engineering Department, University of Windsor, Ontario, N9B 3P4, Canada.

laboratory test under a variety of simulated environments; (b) in a statistical study of an operating component; or (c) in the observation of a natural phenomenon (e.g., ice and rock deformation). This could involve measuring the specimen length under a sustained load at elevated temperatures, recording the creep life time of identical components made from different materials in a machine, or studying geographic maps drawn at different periods of time. The creep properties of a material also depend on its operating environment and may differ markedly from those properties determined in vacuum. (They can be either worse or better depending on the material, its environment, and the interaction between them.)

Over the years the data in the literature have shown that all three stages of creep deformation are interrelated, and information on the early stages, i.e., the primary and secondary stages, can be used to predict the final fracture properties (Ref 4-6). As discussed later in this paper, studies on the creep of pure metals and solid-solution alloys can provide an important understanding of creep mechanisms and provide important "clues" to high-temperature alloy design since the alloy matrix plays a major role in determining the creep resistance of both dispersion-strengthened (DS) alloys and metal-matrix composites (MMCs).

As a natural phenomenon, creep has existed since the creation of solid matter that was subject to applied forces. When man was able to produce alloys and pure metals, such as lead, tin, and their alloys, which had low-melting temperatures, these materials were able to change their geometrical shape (i.e., creep) under their own weight (no extra applied force is needed) at ambient temperature. Creep studies became more important after the industrial revolution and attained increasing importance as operating temperatures were increased for better energy efficiencies. Much of the creep work concentrated on empirical studies and materials characterization. Creep data have been measured for a wide range of engineering materials over a period of about one century. However, the creep mechanism studies have lagged far behind advances in the empirical studies and the technological development of high-temperature alloys (Ref 1, 7-11). Development of high-temperature alloys, in the main, has been the result of painstaking empirical investigation, and it is really only in retrospect that principles underlying these developments have become gradually evident (Ref 1). For example, the empirical recovery creep equation in its present form was obtained two decades ago, but until very recently, there was no satisfactory mechanistic explanation. Often a mechanistic study can provide information useful in technological development, and instances of this can be found in many science and engineering disciplines.

This paper discusses important recent advances in creep of alloys, concentrates on the general aspects and technical importance of the phenomenon, and illustrates this by examples of industrial applications and natural deformation phenomena involving creep. The development of superalloys for gas turbine engine (Ref 7-11), the sintering and hot isostatic pressing (HIP) of powder metallurgy (P/M) compacts (Ref 12-15), and the modeling of the movement of geological formations (e.g., icebergs and the earth mantle) are all dependent on a knowledge of creep (Ref 16, 17). Considerable data has been compiled on the general aspects of creep deformation (Ref 16-19) and on the creep properties of various metals, alloys, intermetallic compounds, carbides, oxides, nitrides, and other ceramics (Ref 20-24), although the mechanisms of creep need to be studied further and improvements are needed in mechanistic modeling. Despite their obvious disadvantages at high temperatures, such as high vapor pressure, lack of oxidation resistance, and lack of resistance to nitrogen (in air) and possibly to carbon and to sulfur (in chemical plant applications), metals are still the principal materials used to carry tensile stress at high temperatures (Ref 25). Various surface coatings have, however, been developed to improve this situation with respect to aggressive creep environments (Ref 26). Thus, this review concentrates mainly on recent developments in creep of metallic materials although other materials are also referred to for comparative purposes.

2. General Aspects of Creep

The creep behavior of a given material is, in general, determined by three factors: (a) the intrinsic properties of the material (atomic bonding, melting temperature, elastic modulus, and activation energy for diffusion—they are interrelated); (b) its microstructural features (chemical composition, phase microstructure, and grain size—these factors can be changed by metallurgical processing); and (c) the operating environment (temperature, applied stress, and test media, such as gas or fluid types). Once a relationship is established among the creep behavior, these material properties, and environmental factors by means of a creep study, it can be used as a guide to material selection, design, and processing for a specific operating environment. Improved creep resistance can be obtained by a proper combination of those material properties, which can be adjusted through a proper choice of materials, and an application of a variety of metallurgical processes, such as alloying additions, controlled casting, mechanical processing, heat treatment, and powder metallurgy, in order to optimize the microstructural features. From these accumulated data on alloy development and mechanical property measurements, some general guidelines, the Honeycombe rules (Ref 27), have been put forward as an aid in the development of creep resistance in materials. These rules follow.

Rule 1. Creep resistance at a given temperature is higher in metals and alloys of high melting point because a metal of high melting point has a lower rate of self-diffusion (with a higher activation energy for self-diffusion) at a specific temperature than a metal of lower melting point. As the rate of dislocation climb is proportional to the rate of self-diffusion, this process, i.e., climb, will be more difficult in a metal of higher melting point. The limiting temperature below which climb cannot occur readily (i.e., atomic self-diffusion is negligible) is about 0.5 T_m, where T_m is the melting (or decomposition) temperature in kelvin. This relationship can be shown from a thermodynamic consideration of the atomic self-diffusion process (Ref 18).

Rule 2. Creep resistance is greater in a matrix of low stacking fault energy (SFE) (creep rate is proportional to the third power of the SFE (Ref 1, 28-30), because the dislocations are dissociated and thus find it more difficult to cross-slip and climb in order to avoid obstacles. The stacking fault energy of a pure metal can be lowered by solute additions. For this purpose,

solutes of high valency are the best additions because they more readily increase the electron to atom ratio and thus decrease the stacking fault energy. Fortunately, such solutes also tend to raise the flow stress more markedly than solutes of lower valence.

Rule 3. Solid-solution hardening can provide a useful contribution to creep resistance and is best achieved by the use of solutes that differ markedly in atomic size and valency from the parent metal. Unfortunately, such solutes do not exhibit extensive solid solubility, and thus their use as solid-solution hardeners is limited.

Rule 4. Long-range order in solid solutions provides a further contribution to the creep strength of solid solutions because the superlattice dislocations are paired to preserve order across the slip plane and are thus similar to extended dislocations.

Rule 5. Precipitates are essential to further increase the creep strength of a solid solution. The Orowan (precipitate strengthening) theory provides an estimate of the critical spacing of a dispersion for the optimum strength as that which is just small enough to prevent dislocations from bowing around the particles ($\sim 10^{-8}$ m). Unfortunately, such fine dispersions are usually not stable at high temperature because diffusion of the elements from the precipitates to the matrix allows coarsening (Ref 31-35). This can be minimized in several ways (Ref 34, 35), namely (a) by choosing elements in the precipitate that diffuse slowly (i.e., have a low diffusion coefficient); (b) by using a dispersed phase that is practically insoluble in the matrix so that the resolution of fine particles and the growth of coarser particles is slow (low solid solubility); and (c) by selecting a precipitate that is crystallographically closely matched to the matrix and remains coherent longer (low interfacial energy).

Rule 6. Precipitates are used in association with crystal defects. Some precipitates form more readily than others on dislocations and thus are important sources of strengthening, both at low and elevated temperatures. Precipitates that form during creep are particularly useful if they nucleate on dislocations. Nucleation in association with stacking faults is another form of strengthening. Precipitation at grain boundaries is useful in reducing grain-boundary sliding, but in many cases this leads to early cavity formation and premature intergranular cracking. High creep strength is thus often achieved, but at the expense of creep ductility. It is possible that grain boundary precipitates with low energy interfaces with the matrix are less likely to cause intergranular failures.

As shown by the preceding discussion, numerous empirical studies have been utilized to make high-temperature superalloys and other engineering materials a reality. Due to its economic and academic importance, and a need for a wide range of structural materials for various engineering applications at high temperatures, creep is receiving increasing attention, as can be seen from the ASM seminars on "Deformation, Processing, and Structure" (Ref 36), and "Flow and Fracture at Elevated Temperatures" (Ref 37), and the Institute of (Metals) Materials (the Swansea) creep conferences (Ref 38-42). In spite of extensive studies, our understanding of creep is far from complete, and the creep properties of engineering materials can still be further improved. This is seen from the early development of the time law for creep, which was based upon the shape of the creep strain-time curves (Ref 18, 43) to the recent creep models based on more detailed microstructure observations and micromechanical mechanisms (Ref 44, 45).

3. Creep of Single-Phase Materials

3.1 *Class I and Class II Creep Behavior*

Researchers have been concentrating their activities in two major areas with respect to the creep mechanisms of single-phase materials (e.g., pure metals and solid-solution alloys): (a) the applied stress and test temperature dependence (i.e., test conditions); and (b) the microstructure dependence (of material properties) of steady-state creep rate. The creep behavior of single-phase crystalline materials has been classified into two categories (Ref 1, 44, 46), class I ($n \cong 3$) and class 2 ($n \cong 5$), in terms of the stress exponent, n, of steady-state creep rate, $\dot{\varepsilon}$. The stress exponent, n, characterizes the rate determining mechanism during creep deformation. The stress exponent, n, is given by a power-law creep equation, $\dot{\varepsilon}_s = \dot{\varepsilon}_0 \sigma^n$, where $\dot{\varepsilon}_0$ is a constant and σ is the applied stress.

The mechanism for class I creep behavior is a viscous glide of dislocations dragging solute atmosphere along their glide path. This class I behavior has been modeled fairly well over the past four decades (Ref 43, 47-56) by considering diffusion associated with a moving potential wall, drag of a Cottrell atmosphere or a Snoek atmosphere by a dislocation, and other solute effects on dislocation motion. A simple explanation of the class I creep was given by Weertman (Ref 57) as follows. When a pure metal is alloyed, a variety of solute mechanisms come into play, which can hinder the motion of dislocations across their slip planes. When a dislocation drifts under the action of an applied stress, σ, by dragging an impurity atmosphere with it, the dislocation velocity, v, is given by the equation, $v = \sigma b / A_v$, no matter which of the solute dragging mechanisms is operative. (In this equation, b is the magnitude of Burgers vector, and A_v is a temperature-dependent constant whose exact value depends on the particular mechanism that controls the dislocation motion.) The steady-state creep rate is given by the Bailey-Orowan equation, $\dot{\varepsilon} = \alpha_1 b \rho v$, where α_1 is a constant about unity, and ρ is the dislocation density. The dislocation density, ρ, in a stressed crystal is given by the Taylor equation, $\sigma = \alpha_2 M \mu b \rho^{1/2}$, where M is the Taylor factor, and μ is the shear modulus. Combining the above three equations, one obtains the following equation for the creep rate: $\dot{\varepsilon}_s = \alpha_3 (\sigma/\mu)^3$ with $\alpha_3 = \alpha_1 \mu / (\alpha_2^2 M^2 A_v)$.. The third power stress dependence of the creep rate is also called the natural law for creep (Ref 57) and is a characteristic feature for creep of class I alloys.

Class II creep is believed to be controlled by a recovery process (dislocation climb) carried out by vacancy diffusion. This view is supported by the experimental results, which show that the activation energy for high-temperature creep is equal to the activation energy for vacancy diffusion in the materials (Ref 58-66), and that for creep of various crystals, the activation volume for creep is similar to that for self-diffusion, indicating a creep mechanism involving vacancies (Ref 60). Thus the temperature dependence of class II creep rate should follow the Arrhenius relationship, which contains a Boltzmann factor (Ref 67-69). That is, $\dot{\varepsilon}_s \propto \exp(-Q/kT)$, where Q is the activation

Table 1 Stress exponent and activation energy values for lattice mechanisms

Mechanism	Stress exponent, n	Activation energy, Q	Ref
Dislocation glide and climb, controlled by climb	4.5	Q_v	Weertman (61, 72, 73)
Dislocation glide and climb, controlled by glide	3	Q_{ci}	Weertman (74)
Dissolution of dislocation loops	4	Q_v	Chang (75)
Dislocation climb from Bardeen-Herring sources	3	Q_v	Nabarro (76)
	5	Q_p	Nabarro (76)
Nonconservative motion of jogged screw dislocations	3	Q_v	Barrett and Nix (77)
Nabarro-Herring creep at subgrain boundaries	3	Q_v	Friedel (48)
Climb of dislocations in 2-dimensional subgrain boundaries	3	Q_v	Ivanov and Yanushkevich (78)
Climb of dislocations in subgrain boundaries of finite width	4	Q_v	Blum (79)
Recovery creep, slip distance is independent of mesh size	4	Q_v	Lagneborg (80, 81)
Recovery creep, including distribution of dislocation link lengths	3 to 5	Q_v	Öström and Lagneborg (82, 83)
Network coarsening by jog-controlled climb	3	Q_v	Gittus (84, 85)
Climb of dislocation links within a 3-dimensional network. Average slip distance equals mesh spacing of network	3	Q_v	Evan and Knowles (63, 64)
	5	Q_p	Evan and Knowles (63, 64)
Climb of dislocation links within a 3-dimensional network. Slip distance is independent of mesh size	4	Q_v	Evan and Knowles (63, 64)
	6	Q_p	Evan and Knowles (63, 64)
Dislocation link collision with a 3-dimensional dislocation network	3	Q_v	Ardell and Przystupa (86)
Dislocation climb of extended dislocations	3 to 5	Q_v	Kong and Li (29, 30)
Dislocation link length statistics for a 3-dimensional dislocation network	3	Q_v	Shi and Northwood (87)

Note: $p = 0$.

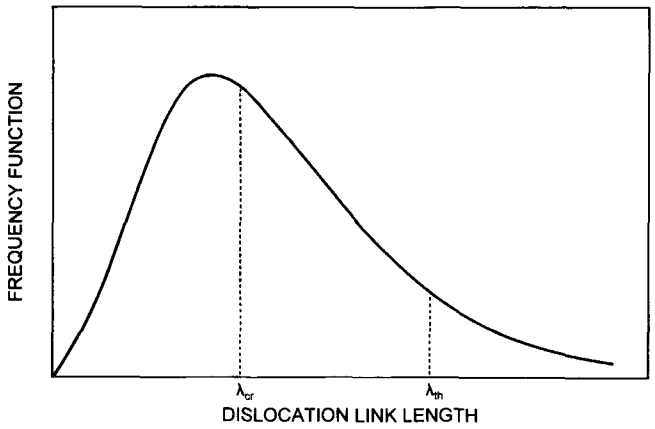

Fig. 2 Dislocation link length distribution showing a typical frequency function, $\phi(\lambda)$, with a critical link length, λ_{cr}, and a threshold link length, λ_{th}.

energy for the appropriate diffusion process, k is the Boltzmann constant ($k = 1.381 \times 10^{-23}$ J/K), and T is the absolute temperature. The empirical constitutive equation was established to describe the power-law creep (Ref 62, 70, 71), although the recovery creep process has not yet been analyzed satisfactorily (Ref 22). In order to model the recovery rate process during elevated temperature creep deformation, the following three factors should be taken into account: (a) the configuration of dislocations and the character of their motion, (b) the forces acting upon dislocations, and (c) the sources and sinks of vacancies.

3.2 *Creep Mechanisms for Single-Phase Materials*

In terms of microstructure, grain size is an important factor in polycrystals, such as alloys and ceramics. In polycrystals, creep is a far more complex phenomenon since the onset of diffusion simultaneously makes a large number of mechanisms of deformation available in addition to dislocation glide and climb. Both lattice mechanisms and boundary mechanisms are operating during high temperature creep deformation. An examination of more than 20 mechanisms by Cannon and Langdon (Ref 23, 24) led to an expression for the steady-state creep rate:

$$\dot{\varepsilon}_s = \frac{ADμb}{kT}\left(\frac{b}{d}\right)^p\left(\frac{\sigma}{\mu}\right)^n \quad \text{(Eq 1)}$$

where A is a dimensionless constant, D is the appropriate diffusion coefficient, d is the grain size, and p is the exponent of the inverse grain size. The diffusion coefficient is:

$$D = D_0 \exp\left(\frac{-Q}{kT}\right) \quad \text{(Eq 2)}$$

where D_0 is a frequency factor. For lattice mechanisms of creep, which are based on intragranular glide and climb of dislocation, $p = 0$, and in general the predicted value of n is within the rather limited range from 3 to 4.5 when the activation energy is equal to the value for lattice self-diffusion (or volume diffusion), Q_v, although it is possible to obtain higher values of n at lower temperatures by invoking pipe diffusion with an activation energy of Q_p ($\cong 0.6Q_v$). For boundary mechanisms of creep, $p \geq 1$.

These representative creep mechanisms for both lattice (or volume) and boundary processes are given in Tables 1 and 2, re-

Table 2 Stress exponent, inverse grain size exponent, and activation energy values for boundary mechanisms

Mechanism	Stress exponent, n	Inverse grain size exponent, p	Activation energy, Q	Reference
Lifshitz sliding				
Nabarro-Herring creep, sliding accommodated by volume diffusion	1	2	Q_v	Nabarro (88), Herring (89)
Coble creep, sliding accommodated by grain-boundary diffusion	1	3	Q_{gb}	Coble (90)
Sliding accommodated by intragranular flow across the grains	1	1	Q_{gb}	Crossman and Ashby (91)
Rachinger sliding				
Sliding with a continuous glassy phase at the boundary	1	1	Q_{ph}	Orowan (92)
Sliding accommodated by the formation of grain-boundary cavities, without a glassy phase	2	1	Q_v	Langdon (93)
Sliding accommodated by the formation of triple-point folds, without a glassy phase	3.5	2	Q_v	Gifkins (94)

spectively. These two tables are set up following the format of Cannon and Langdon (Ref 23, 24) with the addition of recently developed models, i.e., the link length distribution model (Ref 83), the dislocation link collision model (Ref 86), a model based on climb of extended dislocations (Ref 29, 30), and the dislocation link length statistics model (Ref 87). In Tables 1 and 2, Q_v, Q_{ci}, Q_{gb}, and Q_{ph} are the activation energies for lattice (volume) self-diffusion, chemical interdiffusion of solute atoms, grain boundary, and grain boundary phase, respectively. Tables 1 and 2 present various selected creep models for different lattice and grain-boundary creep mechanisms and their main parameters, including the stress exponent, n, the inverse grain size exponent, p, and activation energy, Q, for creep.

3.3 *Dislocation Link Length Statistics Model*

The three recently developed models, dislocation link length distribution model (Ref 83), dislocation link collision model (Ref 86), and dislocation link length statistics model (Ref 87), consider a whole spectrum of dislocation link lengths, λ. See Fig. 2 for a typical dislocation link length distribution frequency function, $\phi(\lambda)$. During plastic deformation, there exists a threshold dislocation link length, λ_{th}, which is determined by the applied uniaxial tensile stress, σ, via the equation $\lambda_{th} = 2\mu b/\sigma$ (Ref 83). The threshold link length, λ_{th}, divides the dislocation link lengths into two groups: the mobile dislocations ($\lambda \geq \lambda_{th}$) and the immobile dislocations ($0 < \lambda < \lambda_{th}$). The creep strain is generated by the glide motion of the mobile dislocation links in the distribution. The controlling mechanism for creep is the coarsening of network (immobile) dislocation links by dislocation climb via vacancy diffusion. The coarsening process involves shrinking of shorter links ($\lambda < \lambda_{cr}$) and growth of longer links ($\lambda_{cr} < \lambda < \lambda_{th}$) of network dislocations where λ_{cr} is the critical dislocation link length. The creep deformation is determined by the evolution of this dislocation link length distribution. Both stress and temperature dependence of the creep rate can be obtained from these models (Ref 83, 86, 87). A recent review was made by the present authors of these dislocation network and link length distribution models for creep (Ref 45).

The dislocation link length statistics are based on direct experimental observations by means of transmission electron microscopy, slip lines on polished surfaces, and etch pit techniques of the dislocation microstructure developed during plastic deformation of crystalline materials. It has been shown that dislocations are arranged into complex, tangled, curved, three dimensional network structures, and that their link lengths have a spectrum of lengths (Ref 95-104). In dislocation link length statistics, the dislocation link length is described by a frequency function, $\phi(\lambda)$, where λ is dislocation link length. The frequency function is defined so that the number of dislocation links, ΔN, and the dislocation density, $\Delta\rho$, in the link length interval from $(\lambda - \Delta\lambda/2)$ to $(\lambda + \Delta\lambda/2)$ are given by $\Delta N = \phi(\lambda)\Delta\lambda$ and $\Delta\rho = \phi(\lambda)\lambda\Delta\lambda$, respectively. In their theoretical study, Wang et al. (Ref 104) obtained an analytical expression for the dislocation link length distribution frequency function, namely $\phi(\lambda) = 2\rho(\lambda^2/\lambda_m^2)\exp(-\lambda^2/\lambda_m^2)$, where λ_m is the dislocation link length when $\phi(\lambda)$ has its maximum value.

An analysis of the dislocation link length statistics for the plastic deformation of crystals (Ref 87) gave the following results. (a) The average dislocation link length, $\langle\lambda\rangle$, of a three-dimensional dislocation network is related to the total dislocation density, ρ, by the equation, $\langle\lambda\rangle = [2/(\pi c)]^{1/2}\rho^{-1/2}$, where c is the dislocation network geometry factor. (b) The strain-hardening coefficient, $H = (\partial\sigma/\partial\varepsilon)_t$, is proportional to, and is of the order of, Young's modulus, E for stress change test during steady-state creep. (c) The creep rate is shown to be primarily determined by the recovery rate, $R = -(\partial\sigma/\partial t)_\varepsilon$, which is directly related to the dislocation annihilation rate, $\dot{\rho}_a = -(\partial\rho/\partial t)_\varepsilon$. (d) A creep rate equation, $\dot{\varepsilon}_s \propto M_0(\sigma/\mu)^3$, is also obtained, where M_0 is the dislocation mobility, which is related to the atomic self-diffusion (Ref 87). Other experimental and theoretical studies on recovery creep have also shown that the creep rate is determined by the recovery rate, R, which is related to the dislocation annihilation rate, $\dot{\rho}_a$ (Ref 83, 105-107).

The dislocation link length statistics have also been applied to constant strain rate deformation (Ref 108-110). The main results from these studies follow. (a) The increase in the flow stress, $\Delta\sigma$, associated with an instantaneous strain rate increase, $\Delta\dot{\varepsilon}$, in the imposed constant strain rate, $\dot{\varepsilon}$, at a given temperature will follow the Haasen relationship in that a plot of $(\Delta\sigma/\Delta\ln\dot{\varepsilon})_T$ versus σ is linear with a slope equal to the strain rate sensitivity, $m = (\partial\sigma/\partial\ln\dot{\varepsilon})_T$ (Cottrell-Stokes law, Ref 111, 112). (b) A model based on the dislocation link length statistics for the three-dimensional dislocation network structure produces reasonable predictions of the variation in the strain-rate sensitivity, m, with a range of $0.126 \leq m \leq 0.333$ for constant strain rate test. (c) The values of the parameter, α, in the Taylor equation

(Ref 113, 114), $\sigma = \alpha M \mu b \rho^{1/2}$, agree well with the results from experimental measurements for many crystalline materials (Ref 108). The dynamic effects of strain hardening and recovery processes during elevated temperature plastic deformation of the 310 stainless steel have been analyzed by means of dislocation link length statistics (Ref 109). The main findings follow. (a) The strain-hardening coefficient for an elevated temperature tensile test is given by the equation:

$$\Theta = H - \frac{2\psi(t)}{A_0}\frac{R}{\dot{\varepsilon}} \qquad \text{(Eq 3)}$$

where H is strain-hardening coefficient for low-temperature plastic deformation without recovery, A_0 is a numerical constant about unity, and $\psi(t)$ is dependent on dislocation structure during deformation. (b) For steady-state deformation at elevated temperatures, the Taylor equation, $\sigma = \alpha M \mu b \rho^{1/2}$, can be deduced from this dislocation link length statistic analysis. (c) The dislocation annihilation rate, $\dot{\rho}_a$, has a stronger stress dependence than the recovery rate, R, and strain rate, $\dot{\varepsilon}_s$. The dislocation annihilation rate, $\dot{\rho}_a$, is proportional to the dislocation density, ρ, in the manner $\dot{\rho}_a \propto \rho^m$, where $m = 2$ to 3 and is a constant (Ref 109). Further a theoretical study (Ref 110) extended the mesh length theory of work hardening (Ref 115-118) to elevated temperature plastic deformation by taking into account thermally activated dislocation annihilation (in addition to the mechanically activated annihilation). Thermal annihilation of dislocations is due to dislocation climb via rapid vacancy diffusion. At elevated temperatures, thermal dislocation annihilation further decreases the dislocation trapping parameter, β, which is defined as the fraction of trapped, i.e., not mutually annihilated, dislocations, by an amount, β_T, which is directly proportional to the recovery rate via an equation, $\beta_T = -[2K\psi(t)/A_0](R/\dot{\varepsilon})$, where $K \cong 300$ is a constant (Ref 110). The shear modulus normalized strain-hardening coefficient is then given by the equation, $\Theta/\mu = (\beta + \beta_T)/K$ (Ref 110). This extended strain-hardening coefficient equation applies to both low- and high-temperature plastic deformation of crystalline materials.

3.4 *Grain-Boundary Mechanisms and Creep of Ceramics*

There are two grain-boundary processes for grain-boundary sliding (Ref 119), Lifshitz sliding (Ref 120) (grain-boundary displacement associated with grain elongation), and Rachinger sliding (Ref 121) (grain-boundary displacement not associated with grain elongation). Examples of Lifshitz sliding are: (a) sliding accommodated by either lattice (or volume) or grain-boundary diffusion—Nabarro-Herring creep (Ref 88, 89) ($n = 1$, $p = 2$, $Q = Q_v$) and Coble creep (Ref 90) ($n = 1$, $p = 3$, $Q = Q_{gb}$ or Q_p); and (b) sliding accommodated by intragranular flow across the grains (Ref 91) ($n = 1$, $p = 1$, $Q = Q_{gb}$ or Q_p). Examples of Rachinger sliding are: (a) sliding with a continuous glassy phase at a boundary (Ref 92) ($n = 1, p = 1, Q = Q_{ph}$); and (b) sliding without a glassy phase—sliding accommodated by the formation of grain boundary cavities (Ref 93) ($n = 2, p = 1, Q = Q_v$), and sliding accommodated by the formation of triple-point folds (Ref 94) ($n = 3.5$, $p = 2$, $Q = Q_v$). In the above relationships, Q_{gb} is the activation energy for grain-boundary diffusion, and Q_{ph} is the activation energy for diffusion through a grain-boundary phase.

Analysis of a wide range of experimental data of the creep on ceramic materials has shown two major points (Ref 23, 24). First, there are many similarities between the creep of ceramics and metals. (a) Diffusion creep with a stress exponent of $n = 1$ occurs at low stresses, and power law creep with $n \geq 3$ occurs at high stresses. (b) There is an inverse relationship between the subgrain size and the applied stress, σ. (c) The dislocation density within the subgrains varies with σ^2. (d) There is a contribution from grain-boundary sliding (GBS), which increases with a decrease in stress and/or grain size. Second, the major differences between the creep of ceramics and the creep of metals are an enhanced role for diffusion creep in ceramics and the power-law creep regime, in which ceramics divide into two categories with stress exponents of ~5 and ~3, respectively. The behavior with $n \cong 5$ is interpreted as fully ductile behavior as in pure face-centered (fcc) metals, and the behavior with $n \cong 3$ is interpreted as dislocation climb from Bardeen-Herring sources (dislocation multiplication sources operated via dislocation climb) (Ref 76, 122), under conditions where there is either a lack of five independent slip systems and general inhomogeneous deformation or, if five independent slip systems are available, there is a lack of interpenetration of these systems. The obvious inference from their microstructure is that boundary mechanisms play a more important role in the creep of ceramics than of metals (Ref 24). This would be in accordance with the inherently lower mobility of dislocations in ceramics as evidenced by the Peierls-Nabarrao stress (a periodic lattice resistance force to dislocation glide motion) and with the differences in preparation of metals and ceramics. For instance, metals and alloys are usually cast into ingots, but ceramic products are normally fabricated using powder metallurgy techniques with additives for consolidation. These differences are likely to lead to thicker grain boundary films in ceramics. Therefore, grain-boundary films in ceramics are very important in determining their creep behavior.

4. Creep of Dispersion-Strengthened Alloys

A practical means of improving the creep resistance of the alloy matrix for high-temperature alloys, such as dispersion-strengthened (DS) alloys and metal-matrix composites (MMCs), is by the introduction of a nondeformable second phase (Ref 123-125). Note that the second-phase particles (or reinforcements) are effective sources of creep strength only when they are thermally stable at elevated temperatures. In contrast to pure metals and single-phase solid-solution alloys, the experimental results on dispersion-strengthened (DS) alloys have shown two general characteristics, namely much higher apparent creep stress exponents, n, and activation energies, Q_c. For example, n values of 7 to 75 and apparent activation energies 2 to 3 times that for self-diffusion have been reported for precipitation and/or oxide-dispersion-strengthened (ODS) nickel-base alloys (Ref 125-129). The activation energies for self-diffusion and those for creep of metals and other materials are tabulated in many publications (Ref 22, 130-133).

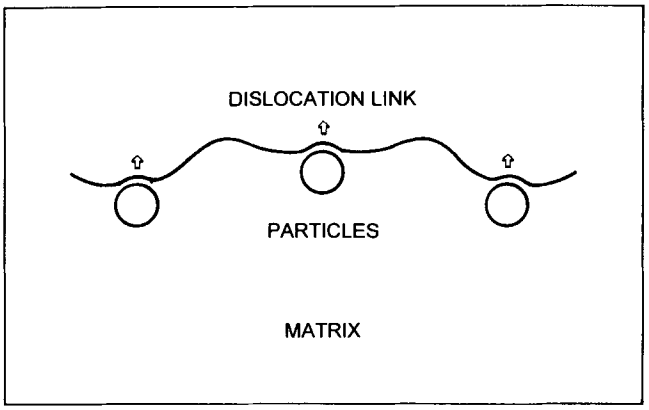

Fig. 3 Attractive particle-dislocation interaction showing a dislocation climb over three particles that are softer than alloy matrix. A part of the dislocation link is still attracted to the particles when the dislocation link is moving forward in the direction indicated by the arrows.

4.1 *Particle-Dislocation Interactions*

There have been many studies on the creep mechanisms of DS alloys. Early studies showed that the increased creep strength in these materials was caused by the resistance to the glide of edge dislocations imparted by the obstacles. Although these obstacles could be circumvented by climb (Ref 134), they reduce the recovery rate for dislocations. This, in turn, is due to a decrease of the driving force for the recovery process and of the mobility of the climbing dislocations involved in the process (Ref 135). The dislocation mechanisms considered in these models are first dislocation climb to bypass particles and then opposite sign dislocation pairs annihilation (i.e., the recovery process) (Ref 134, 135). Only edge dislocations are considered in the models because screw dislocations are able to move without vacancy diffusion. The steady-state creep rate will then be governed by the rate of dislocation climb and annihilation (recovery) process. Good agreement between theories and experimental creep results has been found by applying these models to dispersion-strengthened (DS) alloys. These models can account for the very large stress (exponents) of the steady-state creep rate often found for alloys hardened by a nondeformable second phase, such as sintered aluminum powder (SAP) type alloys, Ni-Cr-Al alloys, and an austenitic 20Cr-35Ni stainless steel containing ordered fcc $\gamma' Ni_3(Al,Ti)$ precipitates.

However, the high values found for the apparent activation energy were not considered at that time. Also, the type of interfaces between particles and matrix and the interaction between dislocations and interfaces were not taken into account by these early climb models. It is becoming more apparent that mechanical properties of multiphase alloys are determined by the matrix, the particle type and size, and the interfaces between matrix and particles (Ref 136). Specifically, during elevated temperature deformation, such as creep, interactions between dislocations and particles are very strongly dependent on the type of interfaces. Some of the early ideas about the attractive and repulsive interactions between dislocations and particles (or voids, grain boundaries, and free surfaces) were presented by Friedel (Ref 48). For instance, an attractive particle-dislocation interaction can be found in the case of soft particles or microvoids where dislocations can relax part of their elastic energy. Figure 3 shows schematically the attractive interaction between a dislocation and three soft particles. The type of interfaces between matrix and particles influences the particle-dislocation interactions and thus mechanical properties, especially in elevated temperature deformation where dislocations can either glide or climb to rearrange themselves in order to achieve low energy configurations (Ref 48). Research in this area can provide important clues for alloy development for elevated temperature applications. Consideration should be given to the selection of the optimum combinations of alloy matrix chemical compositions, particles, and processing methods in order to obtain a strong attractive particle-dislocation interaction during elevated temperature deformation. This becomes more evident from the following sections on attractive particle-dislocation interactions for particle reinforced alloys.

4.2 *Threshold Stresses in Dispersion-Strengthened Alloys*

Recent theoretical models on DS alloys utilized three threshold stresses: (a) the stress required to cause dislocation bowing between particles (the Orowan stress), $\tau_0 = 0.84\ \mu b/(\lambda_P - d)$, where λ_P is the planar spacing between particles, and d is the average particle size (Ref 137-139); (b) the extra back stress required to create the additional dislocation line length as the dislocation segment climbs over a particle (the "local climb" stress), $\tau_b = 0.3\ \mu b/\lambda_P$ (Ref 140, 141), and (c) the stress required to detach the dislocation from the particle after climb is completed in an attractive particle-dislocation interaction (the athermal detachment stress), $\tau_d = (\mu b/\lambda_P)(1 - k_R^2)^{1/2}$, where k_R is given by $\Gamma_P = k_R\Gamma$ in the attractive interaction model, with $\Gamma = \mu b^2/2$ and Γ_P are the line energies of the dislocation in the matrix and at the particle interface, respectively. The parameter k_R ($0 \le k_R \le 1$) can be considered a relaxation parameter. For $k_R = 1$, no attraction between the particle and dislocation exists (no relaxation); for $k_R < 1$, an attractive interaction results, which becomes stronger with diminishing k_R (increasing relaxation) (Ref 142-145). These three stresses are the origin of strengthening mechanisms by particles of DS alloys for elevated temperature applications.

Models that take into account the above three threshold stresses have led to the following important findings. (a) The measured threshold stresses for creep in DS alloys are less than the values predicted from the equation of the Orowan stress by a factor ranging from 1.25 to 2.5 (Ref 140, 146). More significantly, it was suggested (Ref 144) that the concept of the Orowan stress may not be applicable to the deformation of DS alloys at high temperatures and low stresses since the moving dislocations can bypass hard particles (by climbing over them) under these experimental conditions. (b) Deformation processes based on dislocation climb alone cannot provide a satisfactory explanation for the creep of DS alloys in terms of a threshold stress. First, although models based on "local" climb (Ref 140, 141) yield threshold stresses, $\tau_{th} \cong 0.3\ \mu b/\lambda_P$, that are in good agreement with those calculated from creep experimental data on DS alloys, "local" climb, if it occurred, would result in a sharp dislocation curvature (at the point where the

dislocation meets the particle) (Ref 147) that can be rapidly relaxed by diffusion, leading to more "general" climb. Second, models based on "general" climb predicted either an insignificant threshold stress, $\tau_{th} \cong 0.04\ \mu b/\lambda_P$ (Ref 141), or a threshold stress that is proportional to the applied stress (Ref 147-149). (c) The possibility that an attractive interaction between dislocations and particles exists is supported both theoretical (the Srolovitz attractive particle-dislocation interaction (Ref 150, 151) and experimental studies (Ref 152-154). For instance, theoretical studies by Srolovitz et al. (Ref 150, 151) show that an attractive interaction between dislocations and incoherent particles would in fact be expected at elevated temperatures because the incoherent interface can relax parts of the stress field of the dislocation by slipping between particle and matrix interfaces (for relaxing shear stresses) and rapid diffusion (for relaxing normal stresses). Transmission electron microscopy (TEM) observations (Ref 152-154) have revealed that the dislocations remain bound to the particles after climb has been completed. It was demonstrated (Ref 142, 143) that such an attractive particle-dislocation interaction in DS alloy leads to a well-defined threshold stress for creep, which must be exceeded in order to detach the dislocation from a particle after climbing. Most recently, it was suggested (Ref 144) that thermally activated dislocation detachment from the dispersed (hard) particle is the rate controlling mechanism in DS alloys and that the climb process can be regarded as sufficiently rapid for dislocations climbing over particles. In this case, creep may occur below the athermal "detachment stress."

Circumstantial evidence seems to suggest that the ability of incoherent interfaces to attract dislocations at elevated temperatures may be related to poor bonding across that interface. Carbide strengthened aluminum alloys exhibit a strong asymmetry of the flow stress and the creep strength with respect to the loading direction (Ref 144, 155). At elevated temperatures, the strength is reduced considerably under tension compared to compression (whereas no asymmetry is observed at room temperature). This asymmetry was attributed to carbide decohesion from the matrix under tension (interfacial debonding) and thus points to poor interfacial bonding. This is consistent with the finding that carbides are more beneficial for creep strength than oxides, which do not give rise to this asymmetry effect in elevated temperature strength. Creep strength is here referred to the tensile loading for creep, which is the case for most engineering applications of DS alloys.

4.3 *Dislocation Detachment Creep Model*

Assuming that thermally activated dislocation detachment from the particle-matrix interfaces is the rate controlling mechanism in dispersion-strengthened (DS) alloys and that the dislocation climb process can be regarded as sufficiently rapid, the quantitative rate equation developed from this model does not include a "true" threshold stress (Ref 144) and has the form of an Arrhenius expression, namely:

$$\dot{\varepsilon} = \dot{\varepsilon}_0 \exp\left(-\frac{E_d}{kT}\right) \qquad \text{(Eq 4)}$$

where $\dot{\varepsilon}_0$ is the reference strain rate, and E_d is the activation energy for dislocation detachment process. Both $\dot{\varepsilon}_0$ and E_d have been calculated from the model. The reference strain rate, $\dot{\varepsilon}_0$, was estimated by applying nucleation theory (Ref 156). The result is $\dot{\varepsilon}_0 = 3D_v\lambda_P\rho_m/b$, where λ_P is the mean free path between the obstacles, and ρ_m is the mobile dislocation density. An approximate analytical expression for the activation energy for dislocation detachment, E_d, was obtained by analyzing the energetics of dislocation detachment process from an attractive dispersed particle. The passage of a dislocation through a uniform array of spherical particles of radius, r, and spacing, λ_P, was considered in the model analysis. The activation energy for dislocation detachment, E_d, is approximately given by the expression $E_d = \mu b^2 r[(1 - k_R)(1 - \tau/\tau_d)]^{3/2}$. Where the applied shear stress, τ, is equal to or larger than the "athermal detachment stress," τ_d, thermal activation is not necessary to detach the dislocation from the particle. When, however, the applied stress, τ, is smaller than τ_d, the dislocation will reach an equilibrium position at the particle depending upon the applied stress, the line energy of dislocation, and the strength of the dislocation-particle interaction. A finite activation energy for detachment, E_d, has then to be supplied in order to enable dislocation detachment from the attractive dislocation-particle interaction (Ref 144).

The quantitative creep rate equation (Eq 4) developed by Rösler and Arzt (Ref 144) from this model has been compared to the experimental creep data of some DS alloys, such as tungsten wire filaments strengthened by dispersions of potassium vapor-filled bubbles, DS nickel-base superalloy Inconel MA6000 strengthened in addition by yttria (Y_2O_3) dispersoids, fine-grained aluminum strengthened by aluminum carbide (Al_4C_3) and aluminum oxide (Al_2O_3) particles, and rapidly solidified Al-8Fe-4Ce alloy strengthened by $Al_{10}Fe_2Ce$ and $Al_{13}Fe_4$ particles. In all these cases, except fine aluminum strengthened by Al_4C_3 and Al_2O_3 particles (which may be due to grain-boundary effects), good agreement was found between theory and experiment. Based on this theoretical work, suggestions were made as to suitable avenues for alloy development. Obviously, particular attention should be paid to the properties of the particle-matrix interface. A high degree of dislocation relaxation can only be achieved at an incoherent interface with a high specific energy. It is expected from the model that thermally stable bubbles should be the most effective barriers for the motion of dislocations at high temperature since the line energy relaxation should be maximum at this instance. The lowest attainable relaxation factor is $k_R \cong 0.77$. This implies that the high-temperature strength imparted by any particle dispersion cannot exceed about 60% of the Orowan stress, $\tau_d = \tau_0(1 - k_R^2)^{1/2}$. The model also suggests that carbide dispersoids in aluminum alloys are about equally efficient as pores and are more beneficial for creep strength than oxides. This is related to interfacial bonding, which can be affected by the respective chemical compositions and the processing route(s) utilized.

The difference between the elevated temperature creep behavior of precipitate or dispersion-strengthened materials was discussed in terms of the dislocation detachment creep model for the attractive particle-dislocation interaction (Ref 144). In general, precipitation-hardened alloys behave like materials without attractive interaction whereas dispersion-strengthened alloys, produced for instance by mechanical alloying, behave

like materials with a strong attractive particle-dislocation interaction. An important difference between the two particle types is that precipitates, unlike particles dispersed by mechanical means, have to overcome a nucleation energy barrier and are thus forced to form low energy (i.e., strong bonded) phase boundaries (interfaces). Weakly bonded interfaces are needed, however, to allow for the relaxation of the dislocation stress field by atomic rearrangements and fast diffusion along the interface. This may be the reason why small precipitates appear to be less capable of relaxing the line energy of dislocations than small dispersoids. In addition, incoherency across the interface can lead to some degree of dislocation core spreading once the dislocation has reached the particle. This would not be possible at a strongly bonded coherent interface where crystal periodicity has to be maintained. While the detailed understanding of the particle-dislocation interactions at high temperature is certainly not very far advanced, it does appear that on the basis of varying degrees of interfacial bond strength and particle coherency, the creep behavior of the whole class of particle-strengthened materials may be reasonably understood and possibly predicted. This in itself may constitute an important advance over climb theories where the type of interface does not play a role in determining dislocation kinetics and the elevated temperature strength (Ref 144).

There is an important consequence when using creep Eq 4 for extrapolating creep data into regions where experimental data are not available. The shape of the curves of $\log(\dot{\varepsilon}/\dot{\varepsilon}_0)$ versus $\log(\sigma/\sigma_d)$ suggests that only materials with highly attractive dispersoids ($k_R < 0.9$) show "threshold-like" behavior. That is, in terms of conventional threshold stress concept, when the applied stress is less than the threshold stress, the creep rate is negligible. In general, caution should be taken when using a "threshold stress" concept because it may result in serious overestimates of the creep strength at low strain rates (or low applied stresses). This danger may be averted by using the dislocation detachment model based creep rate Eq 4 obtained by Rösler and Arzt (Ref 144).

The above discussed dislocation detachment creep model developed by Rösler and Arzt (Ref 144) was also correlated with available creep data for aluminum alloys strengthened by Al_4C_3 and Al_2O_3 particles, namely alloys Al-2.5, Al-10.0, IN9021, and IN9052 by Orlová and Cadek (Ref 145). Although the model requires an applied stress-dependent apparent activation energy for creep, the stress dependence of creep rate can be satisfactorily accounted for even when this activation energy is stress independent, assuming a strong stress dependence of the per-exponential structure factor, i.e., of the mobile dislocation density. On the other hand, the model is not able to account for the temperature dependence of creep rate if the temperature dependence is much stronger than that of the coefficient of lattice diffusion (a higher activation energy) as is usually the case with alloys strengthened by incoherent particles in which the attractive particle-dislocation interaction can be expected. Orlová and Cadek (Ref 145) suggested that the interpretation of creep in IN9021 alloy in terms of interface controlled diffusional transport of matter may be taken as an alternative to that based on the thermally activated detachment control.

5. Creep of Metal Matrix Composites

Mohamed et al. (Ref 125) recently reviewed creep data of several discontinuous SiC-Al MMCs (whisker and particulate, with Al-Li, Al2124, and Al6061 alloy matrix and reinforcements where the volume or weight fraction of SiC_w or SiC_p ranges from 15 to 30%, and test temperature ranges from 450 to 866 K). The creep behavior of discontinuous SiC-Al MMCs is similar to that of DS alloys in regard to the high values of the stress exponents (the stress exponent n in these composites ranges from about 7 to 25) and the high value of the apparent activation energies, which is much higher than that for self-diffusion in aluminum. An experimental study has shown that the creep of a discontinuous SiC-Al MMC, like that of some DS alloys, exhibits an increase in the stress exponent with decreasing applied stress.

The similarity in creep characteristics between discontinuous SiC-Al MMCs and DS alloys suggests that the creep behavior of the former, like that of the latter, may be explained in terms of a threshold stress for creep. However, by using the various threshold stress models proposed for DS alloys, Mohamed et al. (Ref 125) showed that the threshold stresses introduced by SiC reinforcement are much smaller than those estimated from experimental data. As noted by Mohamed et al. (Ref 125), the creep behavior of discontinuous SiC-Al MMCs is not entirely consistent with the assumptions and predictions of the shear lag models (Ref 157-164), and finite element continuum treatment (Ref 165, 166). For instance, in both the shear lag model (Ref 159, 160) and the finite element continuum treatment (Ref 165), the stress exponent for creep in the composite is equal to that for creep in the unreinforced matrix, whereas experimental results have shown a much larger stress exponent for composites than for their matrices. However, the results of the models and the treatment have provided new insight into the process of load transfer from the matrix to the fiber, the state of stress within a fiber, internal stress distributions in the matrix, the origin of the lower creep rates in discontinuous MMCs, and the role played by reinforcement phase geometry in affecting the overall deformation rate. Further development and extension of the above models and treatment to address in detail important issues, such as void formation and debonding occurrence for different types of interfaces, should lead to increased understanding of high-temperature strengthening in discontinuous composites (Ref 125). Also, studies on how the fiber alignment and particle geometry with respect to loading direction affects the stress distribution in both matrix and reinforcement should provide useful information in material design and processing methods, such as obtaining optimum reinforcement geometry and distribution.

A comparison between detachment stresses, τ_d, for oxide particles and creep threshold stress, τ_0, for a SiC_p-Al alloy 6061 was made by Mohamed et al (Ref 125) and based on the suggestion that the oxide particles, present in the aluminum alloy matrix as a result of manufacturing the composite by powder metallurgy, serve as effective barriers to dislocation motion and give rise to a threshold stress for creep. While the values of τ_d are, in general, close to the values of τ_0, the dependence of τ_0 on temperature is stronger than that of τ_d. (τ_d decreases from 8.65 MPa, 845 MPa to 8.24 MPa, and τ_0 decreases from 10.64 MPa,

8.56 MPa to 7.08 MPa, when T increases from 618 K, 648 K to 678 K, Ref 125.) Examination of the relationship between τ_0 and T led to the empirical equation, $\tau_0/\mu = A_0\exp(Q_0/kT)$, where A_0 is a constant, and Q_0 is an energy term. The origin of the temperature dependence of creep threshold stress, τ_0, is at present not clear, and further creep measurements and models are needed to resolve this issue.

A further analysis was made of the creep data for 14 Al-SiC MMCs (whisker and particulate) with Al2024, Al2124, and Al6061 alloy matrices and reinforcements with volume fractions of SiC_w or SiC_p ranging from 10 to 30% and test temperatures in the range from 503 to 798 K by González-Doncel and Sherby (Ref 167). These tests were aimed at establishing a relationship between strength and microstructure and test conditions (strain rate and temperature) for MMCs. The flow stress of these MMCs depended on the test temperature and the morphology of the reinforcing phase. The strength of the whisker materials was higher (by a factor of 2) than that of the particulate materials at any given temperature. Assuming that creep of Al-SiC composites is controlled by lattice self-diffusion in the aluminum matrix under constant structure after incorporation of a threshold stress, σ_0, a good correlation can be achieved for all the data when the lattice diffusion-compensated strain rate, $\dot{\varepsilon}/D_L$, is plotted as a function of the elastic modulus-compensated effective stress, $(\sigma - \sigma_0)/E$. The calculated threshold stress, σ_0/E, decreases linearly with increasing temperature, and it is higher for the whisker-reinforced composites than for the particulate composites. The temperature above which the threshold stress disappears is very similar for both composites (between 733 and 743 K). For the whisker composites, the σ_0/E value is essentially independent of the direction of testing. The threshold stress is not well understood and cannot be explained by contemporary dislocation models involving dislocation bowing or unpinning around particle sites. The observed interparticle-interwhisker spacing, λ_s, is shown to influence the creep rate in the same way as observed for mechanical alloyed (MA) Al-base materials.

The analysis in Ref 167 also established a criteria for predicting the elevated mechanical behavior of MMCs and understanding the microstructural features that are important in determining their strength. The overall prediction of the flow stress for the Al-SiC composites is:

$$\frac{\sigma}{E} = \left(\frac{\dot{\varepsilon}b^2}{AD_L}\right)^{1/8}\left(\frac{b}{\lambda_s}\right)^{3/8} + \left(\frac{\sigma_0}{E}\right)_0\left(1 - \frac{T}{T_c}\right) \qquad \text{(Eq 5)}$$

where A is a material constant dependent on the stacking fault energy ($A = 10^9$ for aluminum), λ_s is the subgrain size or barrier spacing (whichever is smaller), $(\sigma_0/E)_0$ is modulus-compensated threshold stress at $T = 0$ K, and T_c is the lowest temperature at which the threshold stress is zero. T_c and $(\sigma_0/E)_0$ for Al-SiC MMCs are $T_c = 743$ K and $(\sigma_0/E)_0 = 3.53 \times 10^{-2}$ for whiskers; and $T_c = 733$ K and $(\sigma_0/E)_0 = 2.02 \times 10^{-3}$ for particles (Ref 141). Thus, if the effective barrier spacing is known (through microscopy), and the values of $(\sigma_0/E)_0$ and T_c are known (through strain-rate change tests at two temperatures), the flow stress can be predicted at any given strain rate and temperature for a given Al-SiC material (Ref 167).

In summary, Mohamed et al. (Ref 125) concluded that despite the important contributions of the results of recent studies on discontinuous SiC-Al MMCs, additional experimental and analytical work is still needed in order to (a) examine whether the increase in the stress exponent for creep with decreasing the applied stress represents a genuine creep characteristic in these materials; (b) investigate whether the concept of a threshold stress for creep is capable of accounting for the high apparent stress exponent for creep and the high apparent activation energy in several discontinuous SiC-Al MMCs containing different matrices and different reinforcement configurations and shape; (c) determine whether interfacial debonding occurs; if it occurs, examine its effect on the power law creep, and study the interface during creep deformation for different types of reinforcements and matrices, as well as reinforcement shape and its arrangement, and (d) study dislocation behavior in the composites and identify the nature and type of particles that may interact with dislocations.

6. Role of Alloy Matrix in Creep Strength

Another popular line of study is the role of the alloy matrix in creep behavior of DS alloys (Ref 168-170). In these studies, the resisting stress concept has been utilized and extended. An assumption is made that the creep rate is determined by a net stress, which is equal to the applied stress minus total resisting stresses arising from solid solution atoms and particles. The experimental data were evaluated for many DS nickel-base superalloys with various levels of matrix solid-solution strengthening. The alloys examined include thoria (ThO_2) dispersed TD-nickel; the oxide-dispersion-strengthened (ODS) mechanical alloys MA 754 and MA 753 (International Nickel Company, London, UK); the ordered fcc $\gamma' Ti_3Al$ strengthened superalloys Udimet 700 (Special Metals Corporation, Ann Arbor, MI), Nimonic 115 (Henry Wiggins Limited U.K.), and MAR M200 (Martin-Marietta Inc., Bethesda, MD); and mechanical alloy MA6000E (International Nickel Company, London, U.K.) strengthened by inert yttria (Y_2O_3) dispersoids and a high-volume fraction of $\gamma' Ti_3Al$ precipitates. A generalized expression has been developed for the creep rates that separates the matrix contributions from the particle contributions to the resisting stress and creep strength of these alloys. This generalized creep rate equation is:

$$\dot{\varepsilon}_s = A_p(1 - k_s)^N\left(\frac{\sigma - \sigma_p}{E}\right)^N \exp\left(-\frac{Q}{RT}\right) \qquad \text{(Eq 6)}$$

where A_p is a structure-dependent parameter; k_s is a proportionality constant, which is in the range from 0 to 1 and increases in magnitude with the extent of solid-solution strengthening in the matrix phase; N is a stress exponent; σ is the applied stress; σ_p is the applied-stress-independent average resisting stress due to the strengthening particles; and E is Young's modulus (temperature dependent). A resisting stress component due to the matrix solid-solution phase, which is proportional to the net applied stress experienced by the matrix, is $\sigma_s = k_s(\sigma - \sigma_p)$. The total resisting stress to creep in these particle-strengthened systems is $\sigma_r = \sigma_p + \sigma_s = \sigma_p + k_s(\sigma - \sigma_p)$. The above creep rate equation allows one to express the particle contribution to creep resistance of the alloy through the σ_p term in the resisting stress and through the contribution of the matrix phase through

the $(1 - k_s)^N$ term. It is also shown by Ajaja et al. (Ref 170) that the apparent stress exponent, n, is related to the N and applied stress, σ, by a relation $n \equiv N(1 - \sigma_p/\sigma)$. The larger the ratio σ_p/σ, the more sensitive is the creep rate to changes in the applied stress; this is not desirable in most applications. The apparent activation energy, Q_c, is shown to be related to the temperature dependencies of Young's modulus dE/dT and the particle resisting stress, σ_p, namely $Q_c = Q + f(dk_s/dT, dE/dT, d\sigma_p/dT)$, where Q is defined by the expression $Q \equiv RT^2(\partial \log \dot{\varepsilon}_s/\partial T)_0$, and f is a function of the temperature dependencies of the three parameters, k_s, E, and σ_p.

Ajaja et al. (Ref 170) concluded that the major role of the alloy matrix in the creep behavior of these alloys is in determining the apparent stress dependence of the creep rates. Specifically, the stronger the matrix becomes through solid-solution strengthening, the lower the applied stress dependence of the creep rate of the alloy. Then an alloy with a comparatively strong matrix can be more safely applied to an elevated temperature situation where stress is fluctuating, which is the case for many practical engineering applications. This type of analysis clearly established the role played by solid-solution strengthening of matrix in the overall creep resistance of high-temperature alloys, which are predominantly strengthened by second-phase particles.

From an alloy design point of view, these findings are particularly significant because of the availability of such versatile processes as mechanical alloying (Ref 171-173), which has made possible the development of alloys with tailor-made compositional specifications with controlled amounts of inert dispersed strengtheners. For example, the undesirable high applied stress sensitivity displayed by DS alloys is not an intrinsic characteristic of these alloys but can be changed. In particular, increasing the solid solution strengthening contribution to the creep resisting stress to a level comparable with that of the particle contribution would make this change possible. Decreasing the applied stress sensitivity is of practical value in improving the performance reliability of these alloys under real, in-service conditions where spiked overloads might be expected. The analysis (Ref 170) further indicates that even small amounts of specific elements, e.g., the refractory elements tungsten and molybdenum, could be very potent in improving creep resistance through solid-solution strengthening rather than larger amounts of other elements. A ranking of the solid-solution strengthening potency of the usual alloying elements in these high-temperature alloys, perhaps based on effects related to atomic size misfit, effects related to electron vacancy number differences, or effects related to shear modulus differences (see Ref 174-176), would serve as a useful guideline in particle-strengthened alloy design for better creep resistance through enhanced solid-solution strengthening.

Examples for alloy development in obtaining high tensile strength and good fracture properties by adjusting alloy chemistry can be found for a plain carbon steel with rare earth treatment (Ref 177-179) and a biomedical cobalt-chromium alloy for dental and surgical applications (Ref 180-181). In this alloy development, both solid-solution hardening and particle strengthening were taken into account in preparation of the alloys. For microalloying a plain carbon steel with rare earth elements (Ref 177-179), the aim was to control the microstructure and to modify sulfide inclusions and grain-boundary chemistry, thereby to improve the mechanical and electrochemical properties of the steel. For a biomedical cobalt-chromium alloy development (Ref 180, 181), the chemical compositions were designed according to alloying theory (Ref 182, 183), namely to prevent the formation of topologically close-packed (TCP) phases by using the mean electron-hole number method. Alloying elements, such as tungsten and molybdenum, were added into the alloy as solid-solution hardeners, and chromium was for carbide formation (particle strengthening), ductility, and corrosion resistance. Although these are examples of low-temperature applications, the principles can be extended for alloys designed for elevated temperature applications.

7. Summary and Conclusions

The technological development of high temperature creep-resistant alloys and the mechanistic studies of creep behavior are interrelated (Ref 22-25). This is particularly evident in two areas. Solid-solution strengthening and particle or fiber reinforcement of the matrix are connected to the lattice mechanisms of creep and to the interactions between dislocations and solute atoms, reinforcements, and interfaces. High-temperature creep and superplastic deformation of polycrystalline metallic and especially ceramic materials are linked to the boundary mechanisms of creep with various accommodations (grain-boundary and/or lattice diffusion, grain-boundary glassy phase, intragranular flow across the grains, the formation of grain-boundary cavities, and the formation of triple-point folds) (Ref 184-197).

With respect to modeling of elevated temperature creep of metals and alloys, significant advance has been made recently, such as dislocation link length statistics model, dislocation detachment model, and the resistance stresses model. The dislocation link length statistics model is based on the experimental observations that link lengths are not uniform but rather taken on a whole spectrum of lengths. The results from the dislocation link length statistics model are in good agreement with creep experiments and plastic deformation of single-phase materials in general. But more importantly, the creep rate is determined by the recovery rate. Any factor that reduces the recovery rate (or dislocation annihilation rate) and stabilizes the dislocation network structure, will decrease the creep rate and thereby increase creep resistance. However, details of the dislocation micromechanisms need to be studied carefully in order to study complex engineering alloy systems, such as DS alloys and MMCs.

For multiphase DS alloys and MMCs, the properties of alloy matrix, the interfaces, and the interaction between the matrix and the reinforcements must be considered since all three factors determine the creep properties and elevated temperature strength of these materials (Ref 198-205). Theoretical creep models based on attractive particle-dislocation interactions (dislocation detachment creep model) have demonstrated the importance of the interfaces on creep strength, and have shown that in general noncoherent interfaces with high interfacial energies are a potential source for creep resistance and elevated temperature strength. This arises because the interfaces can partially relax the elastic energy of interacting dislocations,

which are more tightly bonded to the interfaces. Models based on resistance stresses for creep have shown that the elevated temperature strength of the alloy matrix is an important factor in maintaining overall creep resistance and elevated temperature creep performance for dispersion-strengthened alloys. The strengthening effect of the alloy matrix is obtained mainly by alloying with solid solution elements. A comparative increase in strength for the alloy matrix can reduce the stress dependence of the creep rate, i.e., decrease the stress exponent, n, thereby making alloys suitable for a wider range of applied stresses (or stress fluctuating) in practical service.

Examination of some recent experimental creep results for MMCs (mainly aluminum alloy matrix composites) reveal that creep models for DS alloys may be applicable to these materials. However, further work is required to study interfacial debonding for different kinds of reinforcements and matrices and the nature and type of particle-dislocation interactions during creep. These studies can provide information for MMCs fabrication routes and matrix chemical composition and reinforcement selections in order to develop MMCs for elevated temperature applications with a high creep resistance and elevated temperature strength.

Acknowledgment

Funding for these studies was provided by the Natural Sciences and Engineering Research Council of Canada through a research grant (NSERC A 4391) awarded to Professor D.O. Northwood.

References

1. O.D. Sherby and P.M. Burke, Mechanical Behavior of Crystalline Solids at Elevated Temperature, *Prog. Mater Sci.*, Vol 13 (No. 7), 1968, p 323-390
2. E.N. da C. Andrade, On the Viscous Flow in Metals, and Allied Phenomena, *Proc. R. Soc. (London) A*, Vol 84 (No. 567), 1911, p 1-12
3. E.N. da C. Andrade, The Flow in Metals Under Large Constant Stresses, *Proc. R. Soc. (London) A*, Vol 90 (No. 619), 1914, p 329-342
4. F.C. Monkman and N.J. Grant, An Empirical Relationship Between Rupture Life and Minimum Creep Rate in Creep-Rupture Tests, *Proc. ASTM*, Vol 56, 1958, p 593-620
5. F. Dobeš and K. Milicka, The Relationship Between Minimum Creep Rate and Time to Fracture, *Met. Sci.*, Vol 10 (No. 11), 1976, p 382-384
6. C. Phaniraj, M. Nandagopal, S.L. Mannan, and P. Rodriguez, The Relationship Between Transient and Steady State Creep in AISI 304 Stainless Steel, *Acta Metall. Mater*, Vol 39 (No. 7), 1976, p 1651-1656
7. *The Superalloys*, C.T. Sims and W.C. Hagel, Ed., John Wiley & Sons, 1972
8. *Superalloys II: High Temperature Materials for Aerospace and Industrial Power*, C.T. Sims, N.S. Stoloff, and W.C. Hagel, Ed., John Wiley & Sons, 1987
9. T.M. Pollock and A.S. Argon, Creep Resistance of CMSX-3 Nickel-Base Superalloy Single Crystals, *Acta Metall. Mater*, Vol 40 (No. 1), 1992, p 1-30
10. *Powder Metallurgy*, W. Leszynski, Ed., Interscience, 1961
11. G.H. Gessinger, *Powder Metallurgy of Superalloys*, Butterworth, 1984
12. M.F. Ashby, A First Report on Sintering Diagram, *Acta Metall.*, Vol 22 (No. 3), 1974, p 275-289
13. F.B. Swinkels and M.F. Ashby, A Second Report on Sintering Diagram, *Acta Metall.*, Vol 29 (No. 2), 1981, p 259-281
14. E. Arzt, M.F. Ashby, and K.E. Easterling, Practical Applications of Hot-Isostatic Pressing Diagrams: Four Case Studies, *Metall. Trans. A*, Vol 14 (No. 2), 1983, p 211-221
15. A.C.F. Cocks, The Structure of Constitutive Laws for the Sintering of Fine Grained Materials, *Acta Metall. Mater*, Vol 42 (No. 7), 1994, p 2191-2210
16. J.H. Gittus, *Creep, Viscoelasticity and Creep Fracture in Solids*, John Wiley & Sons, 1975
17. J.P. Poirier, *Creep of Crystals: High-Temperature Deformation Processes in Metals, Ceramics and Minerals*, Cambridge University Press, 1985
18. F. Garofalo, *Fundamentals of Creep and Creep-Rupture in Metals*, MacMillan, 1965
19. R.W. Evans and B. Wilshire, *Creep of Metals and Alloys*, Institute of Metals, 1985
20. T.G. Langdon, Grain Boundary Deformation Processes, *Deformation of Ceramic Materials*, R.C. Bradt and R.E. Tressler, Ed., Plenum Publishing, 1975, p 101-126
21. A.G. Evans and T.G. Langdon, Structural Ceramics, *Prog. Mater Sci.*, Vol 2 (No. 3/4), 1976, p 171-441
22. H.J. Frost and M.F. Ashby, *Deformation-Mechanism Maps: The Plasticity and Creep of Metals and Ceramics*, Pergamon Press, 1982
23. W.R. Cannon and T.G. Langdon, Creep of Ceramics, Part I Mechanical Characteristics, *J. Mater Sci.*, Vol 18 (No. 1), 1983, p 1-50
24. W.R. Cannon and T.G. Langdon, Creep of Ceramics, Part II An Examination of Flow Mechanism, *J. Mater Sci.*, Vol 23 (No. 1), 1988, p 1-20
25. A. Kelly and N.H. Macmillan, *Strong Solids*, 3rd ed., Clarendon, 1986, p 223-231
26. *Materials and Coatings to Resist High Temperature Corrosion*, D.R. Holmes and A. Rahmel, Ed., Applied Science, 1978
27. R.W.K. Honeycombe, *The Plastic Deformation of Metals*, 2nd ed., Edward Arnold, 1984, p 393-394
28. F.A. Mohamed and T.G. Langdon, The Transition from Dislocation Climb to Viscous Glide in Creep of Solid Solution Alloys, *Acta Metall.*, Vol 22 (No. 6), 1974, p 779-788
29. Q.P. Kong and Y. Li, On the Climb Process of Extended Dislocations During High Temperature Creep, *Phys. Stat. Solidi, A*, Vol 126 (No. 1), 1991, p 129-134
30. Q.P. Kong and Y. Li, Investigation of the Climb of Extended Dislocations During High Temperature Creep, *Philos. Mag. A*, Vol 68 (No. 1), 1993, p 113-119
31. W. Ostwald, Über die vermeintliche Isomerie des roten und gelben Quecksilberoxyds und die Oberflächenspannung fester Körper, (On the general isomers of red and yellow mercury oxide and the surface tension of solid bodies)*Z. Phys. Chem.*, Vol 34 (No. 4), 1900, p 495-503 (in German)
32. I.M. Lifshitz and V.V. Slyozov, The Kinetics of Precipitation From Supersaturation Solid Solutions, *J. Phys. Chem. Solids*, Vol 19 (No. 1/2), p 35-50
33. C. Wagner, Theorie der Alterung von Niederschlägen durch Umlösen (Ostwald-Reifung), [Theory of aging of precipitates through disolution (Ostwald-Ripening)],*Z. Elektrochem.*, Vol 65 (No. 7/8), 1961, p 581-591 (in German)
34. J.W. Martin and R.D. Doherty, Precipitate Coarsening: "Ostwald Ripening," *Stability of Microstructure in Metallic Systems*, Cambridge University Press, 1976, p 173-244
35. H. Gleiter, Microstructure, *Physical Metallurgy*, 3rd ed., R.W. Cahn and P. Haasen, Ed., North-Holland Physics, 1983, p 649-712
36. *Deformation, Processing, and Structure*, G. Krauss, Ed., American Society for Metals, 1984

37. *Flow and Fracture at Elevated Temperatures*, R. Raj, Ed., American Society for Metals, 1985
38. *Proc. 1st Int. Conf. on Creep and Fracture of Engineering Materials and Structures*, B. Wilshire and D.R.J. Owen, Ed., Pineridge Press, 1981
39. *Proc. 2nd Int. Conf. on Creep and Fracture of Engineering Materials and Structures*, B. Wilshire and D.R.J. Owen, Ed., Pineridge Press, 1984
40. *Proc. 3rd Int. Conf. on Creep and Fracture of Engineering Materials and Structures*, B. Wilshire and D.R.J. Owen, Ed., Pineridge Press, 1987
41. *Proc. 4th Int. Conf. on Creep and Fracture of Engineering Materials and Structures*, B. Wilshire and D.R.J. Owen, Ed., Pineridge Press, 1990
42. *Proc. 5th Int. Conf. on Creep and Fracture of Engineering Materials and Structures*, B. Wilshire and D.R.J. Owen, Ed., Pineridge Press, 1993
43. A.H. Cottrell, Creep, *Dislocations and Plastic Flow in Crystals*, Oxford University Press, 1953, p 195-215
44. S. Takeuchi and A.S. Argon, Steady-State Creep of Single-Phase Crystalline Matter at High Temperature, *J. Mater Sci.*, Vol 11 (No. 7), 1976, p 1542-1566
45. L. Shi and D.O. Northwood, Dislocation Network Models for Recovery Creep Deformation, *J. Mater Sci.*, Vol 28 (No. 22), 1993, p 5963-5974
46. D.O. Northwood and I.O. Smith, Experimental Techniques for Probing the Micromechanisms of Creep: A Review, *Met. Forum*, Vol 8 (No. 4), 1985, p 237-249
47. A.H. Cottrell and M.A. Jaswon, Distribution of Solute Atoms Round a Slow Dislocation, *Proc. R. Soc. (London) A*, Vol 199 (No. 1056), 1949, p 104-114
48. J. Friedel, *Dislocations*, Pergamon Press, 1964, Ch XI, p 303-319; Hardness of a Crystal Containing Uniformly Distributed Impurities or Precipitates, Ch XIV, p 368-384; Formation and Motion of Impurity Clouds, Ch XVI, p 405-414
49. F.A. Mohamed and T.G. Langdon, Creep Behavior of Ni-W Solid Solutions (Communications), *Metall. Trans. A*, Vol 6 (No. 4), 1975, p 927-928
50. F.A. Mohamed and T.G. Langdon, Creep Behavior of Ceramic Solid-Solution Alloys (Discussion and Notes), *J. Am. Ceram. Soc.*, Vol 58 (No. 11-12), 1975, p 533-534
51. S. Takeuchi and A.S. Argon, Steady-State Creep of Alloys Due to Viscous Motion of Dislocations, *Acta Metall.*, Vol 24 (No. 10), 1976, p 883-889
52. S. Takeuchi and A.S. Argon, Glide and Climb Resistance to the Motion of an Edge Dislocation Due to Dragging a Cottrell Atmosphere, *Philos. Mag. A*, Vol 40 (No. 1), 1979, p 65-75
53. R. Fuentes-Sasmlaniego, Theoretical Studies of Diffusional Processes in Solids Under Pressure, Ph.D. thesis, Stanford University, Stanford, CA, 1979
54. J.P. Hirth and J. Lothe, Dislocation—Point-Defect Interactions at Finite Temperatures, *Theory of Dislocations*, 2nd ed., Part 3, John Wiley & Sons, 1982, p 485-694
55. G.A. Henshall and A.K. Miller, Simplifications and Improvements in Unified Constitutive Equations for Creep and Plasticity— I. Equations Development, *Acta Metall. Mater*, Vol 38 (No. 11), 1990, p 2101-2115
56. G.A. Henshall and A.K. Miller, Simplifications and Improvements in Unified Constitutive Equations for Creep and Plasticity—II. Behavior and Capabilities of the Model, *Acta Metall. Mater*, Vol 38 (No. 11), 1990, p 2117-2128
57. J. Weertman and J.R. Weertman, Mechanical Properties, Strongly Temperature-Dependent, *Physical Metallurgy*, 3rd ed., R.W. Cahn and P. Haasen, Ed., North-Holland Physics, 1983, p 1309-1340
58. J.E. Dorn, The Spectrum of Activation Energies for Creep, *Creep and Recovery*, American Society for Metals, 1957, p 255-283
59. D.A. Prokoshkin and E.V. Vasil'eva, Temperature Dependence of Diffusion Rate of Metals, *Dokl. Akad. Nauk SSSR*, Vol 177 (No. 5), 1967, p 1069-1071
60. J.C.M. Li, Kinetics and Dynamics in Dislocation Plasticity, *Dislocation Dynamics*, A.R. Rosenfield, G.T. Hahn, A.L. Bement, Jr., and R.I. Jaffe, Ed., McGraw-Hill, 1968, p 87-116
61. J. Weertman, Dislocation Climb Theory of Steady-State Creep, *Trans. ASM*, Vol 61 (No. 4), 1968, p 681-694
62. A.K. Mukherjee, J.E. Bird, and J.E. Dorn, Experimental Correlations for High-Temperature Creep, *Trans. ASM*, Vol 62 (No. 1), 1969, p 155-179
63. H.E. Evans and G. Knowles, A Model of Creep in Pure Materials, *Acta Metall.*, Vol 25 (No. 8), 1977, p 963-975
64. H.E. Evans and G. Knowles, Dislocation Creep in Non-Metallic Materials, *Acta Metall.*, Vol 26 (No. 1), 1978, p 141-145
65. O.D. Sherby and J. Weertman, Diffusion-Controlled Dislocation Creep: A Defense, *Acta Metall.*, Vol 27 (No. 3), 1979, p 387-400
66. K. Milicka, Constant Structure Creep in Metals After Stress Reduction in Steady State Stage, *Acta Metall. Mater*, Vol 41 (No. 4), 1993, p 1163-1172
67. R.F. Feynman, R.B. Leighton, and M. Sands, The Principles of Statistical Mechanics, *The Feynman Lectures on Physics*, Vol 1, Addison-Wesley, 1963, p 40-1-to 40-10
68. A.S. Krausz and H. Eyring, Deformation in Creep and in Creep Recovery, *Deformation Kinetics*, John Wiley & Sons, 1975, p 180-225
69. U.F. Kocks, A.S. Argon, and M.F. Ashby, Thermodynamics and Kinetics of Slip, *Prog. Mater Sci.*, Vol 19, 1975, p 1-288
70. F.H. Norton, Discussion of Results, *The Creep of Steel at High Temperatures*, McGraw-Hill, 1929, p 67-70
71. J.E. Bird, A.K. Mukherjee, and J.E. Dorn, Correlations Between High-Temperature Creep Behavior and Structure, *Quantitative Relation Between Properties and Microstructures*, D.G. Brandon and A. Rosen, Ed., Israel University Press, 1969, p 255-342
72. J. Weertman, Steady-State Creep Through Dislocation Climb, *J. Appl. Phys.*, Vol 28 (No. 3), 1957, p 362-364
73. J. Weertman, High Temperature Creep Produced by Dislocation Motion, *Rate Processes in Plastic Deformation of Materials*, J.C.M. Li and A.K. Mukherjee, Ed., American Society for Metals, 1975, p 315-336
74. J. Weertman, Steady-State Creep of Crystals, *J. Appl. Phys.*, Vol 28 (No. 10), 1957, p 1185-1189
75. R. Chang, Dislocation Theories of the High-Temperature Creep of Crystalline Solids, *The Physics and Chemistry of Ceramics*, C. Klingsberg, Ed., Gordon and Breach Science Publishers, 1963, p 275-285
76. F.R.N. Nabarro, Steady-State Diffusional Creep, *Philos. Mag.*, Vol 16 (No. 140), 1967, p 231-237
77. C.R. Barrett and W.D. Nix, A Model for Steady State Creep Based on the Motion of Jogged Screw Dislocations, *Acta Metall.*, Vol 13 (No. 12), 1965, p 1247-1258
78. L.I. Ivanov and V.A. Yanushkevich, High-Temperature Mechanism of Steady-State Creep in B.C.C. Metals, *Fiz. Metal. Metalloved.*, Vol 17 (No. 1), 1964, p 112-117
79. W. Blum, Role of Dislocation Annihilation During Steady-State Deformation, *Phys. Stat. Solidi B*, Vol 45 (No. 2), p 561-571
80. R. Lagneborg, Development and Refinement of the Recovery-Creep Theory, *Met. Sci. J.*, Vol 3 (No. 9), 1969, p 161-168
81. R. Lagneborg, A Modified Recovery-Creep Model and Its Evaluation, *Met. Sci. J.*, Vol 6 (No. 7), 1972, p 127-133
82. P. Öström and R. Lagneborg, A Recovery-Athermal Glide Creep Model, *J. Eng. Mater Tech. (Trans. ASME Series H)*, Vol 98 (No. 2), 1976, p 114-124
83. P. Öström and R. Lagneborg, A Dislocation Link Length Model for Creep, *Res Mechanica*, Vol 1 (No. 1), 1980, p 59-79

84. J.H. Gittus, Development of a Theoretical Equation for Steady-State Dislocation Creep and Comparison with Data, *Acta Metall.*, Vol 22 (No. 6), 1974, p 789-791
85. J.H. Gittus, Theoretical Equation for Steady State Dislocation Creep: Effect of Solute Drag, *Acta Metall.*, Vol 22 (No. 9), 1974, p 1179-1181
86. A.J. Ardell and M.A. Przystupa, Dislocation Link-Length Statistics and Elevated Temperature Deformation of Crystals, *Mech. Mater*, Vol 3 (No. 4), 1984, p 319-332
87. L. Shi and D.O. Northwood, On Dislocation Link Length Statistics for Plastic Deformation of Crystals, *Phys Stat. Solidi A*, Vol 137 (No. 1), 1993, p 75-85
88. F.R.N. Nabarro, Deformation of Crystals by the Motion of Single Ions, *Report of a Conference on Strength of Solids*, The Phys. Soc., London, 1948, p 75-90
89. C. Herring, Diffusional Viscosity of a Polycrystalline Solid, *J. Appl. Phys.*, Vol 21 (No. 5), 1950, p 437-445
90. R.L. Coble, A Model for Boundary Diffusion Controlled Creep in Polycrystalline Materials, *J. Appl. Phys.*, Vol 34 (No. 6), 1963, p 1679-1682
91. F.W. Crossman and M.F. Ashby, The Non-Uniform Flow of Polycrystals by Grain-Boundary Sliding Accommodated by Power-Law Creep, *Acta Metall.*, Vol 23 (No. 4), 1975, p 425-440
92. E. Orowan, The Creep of Metals, *J. West Scotland Iron Steel Inst.*, Vol 54, 1946/1947, p 45-96
93. T.G. Langdon, Grain Boundary Sliding as a Deformation Mechanism During Creep, *Philos. Mag.*, Vol 22 (No. 178), 1970, p 689-700
94. R.C. Gifkins, The Grain-Size Dependence of Creep Rate in Recovery Creep, *J. Aust. Inst. Met.*, Vol 18 (No. 3), 1973, p 137-145
95. D.J. Dingley and D. McLean, Components of the Flow Stress of Iron, *Acta Metall.*, Vol 15 (No. 5), 1967, p 885-901
96. A. Odén, E. Lind, and R. Lagneborg, Dislocation Distributions During Creep and Recovery of a 20%Cr-35%Ni Steel at 700 °C, *Proc. of a Meeting on Creep Strength in Steel and High Temperature Alloys*, Iron and Steel Institute, 1970, p 60-66
97. M.R. Staker and D.L. Holt, The Dislocation Cell Size and Dislocation Density in Copper Deformed at Temperatures Between 25 and 700 °C, *Acta Metall.*, Vol 20 (No. 4), 1972, p 569-579
98. J.B. Bilde-Sörensen, Dislocation Link Length Distribution in Creep-Deformed Magnesium Oxide, *Acta Metall.*, Vol 21 (No. 11), 1973, p 1495-1501
99. L.E. Murr and D. Kuhlmann-Wilsdorf, Experimental and Theoretical Observations on the Relationship Between Dislocation Cell Size, Dislocation Density, Residual Hardness, Peak Pressure and Pulse Duration in Shock-Loaded Nickel, *Acta Metall.*, Vol 26 (No. 5), 1978, p 847-857
100. J.D. Parker and B. Wilshire, Rate-Controlling Processes During Creep of Super-Purity Aluminium, *Philos. Mag.*, Vol 41 (No. 5), 1980, p 665-680
101. F.R. Castro-Fernández and C.M. Sellars, Relationship Between Room-Temperature Proof Stress, Dislocation Density, and Subgrain Size, *Philos. Mag. A*, Vol 60 (No. 4), 1989, p 487-506
102. P. Lin, S.S. Lee, and A.J. Ardell, Scaling Characteristics of Dislocation Link Length Distributions Generated During the Creep of Crystals, *Acta Metall.*, Vol 37 (No. 2), 1989, p 739-748
103. B. Bay, N. Hansen, D.A. Hughes, and D. Kuhlmann-Wilsdorf, Evolution of F.C.C. Deformation Structures in Polyslip, *Acta Metall. Mater*, Vol 40 (No. 2), 1992, p 205-219
104. B. Wang, F. Sun, Q. Meng, and W. Xu, An Approach to Mathematical Modeling of Dislocation Link Length Distribution in Metal, *Acta Metall. Sin. A*, Vol 28 (No. 3), 1992, p 100-103
105. S.O. Ojediran and O. Ajaja, The Bailey-Orowan Equation, *J. Mater Sci.*, Vol 23 (No. 11), 1988, p 4037-4040
106. L. Shi and D.O. Northwood, Creep of an AISI 310 Type Stainless Steel and Its Numerical Simulation Using the Öström-Lagneborg Creep Model, *Acta Metall. Mater*, Vol 41 (No. 12), 1993, p 3393-3400
107. L. Shi and D.O. Northwood, Strain-Hardening and Recovery During the Creep of Polycrystalline Magnesium, *Acta Metall. Mater*, Vol 42 (No. 3), 1994, p 871-877
108. L. Shi and D.O. Northwood, On Dislocation Link Length Statistics for Constant Strain Rate Deformation, *Phys. Stat. Solidi A*, Vol 140 (No. 1), 1993, p 87-95
109. L. Shi and D.O. Northwood, On Dislocation Link Length Statistics for Strain Hardening and Recovery During Elevated Temperature Plastic Deformation, *Fourth LEDS Conference*, Winnipeg, Manitoba, 1995
110. D. Kuhlmann-Wilsdorf and L. Shi, Theory of Workhardening Stages, unpublished research, University of Virginia, 1994
111. A.H. Cottrell and R.J. Stokes, Effects of Temperature on the Plastic Properties of Aluminium Crystals, *Proc. R. Soc. (London) A*, Vol 233 (No. 112), 1955, p 17-32
112. J. Weertman and J.R. Weertman, Mechanical Properties, Mildly Temperature-Dependent, *Physical Metallurgy*, 3rd ed., R.W. Cahn and P. Haasen, Ed., North-Holland Physics, 1983, p 1259-1307
113. G.I. Taylor, The Mechanism of Plastic Deformation of Crystals. Part I.—Theoretical, *Proc. R. Soc. (London) A*, Vol 145 (No. 855), 1934, p 362-387
114. G.I. Taylor, The Mechanism of Plastic Deformation of Crystals. Part II.—Comparison with Observations, *Proc. R. Soc. (London) A*, Vol 145 (No. 855), 1934, p 388-404
115. D. Kuhlmann-Wilsdorf, A New Theory of Workhardening, *Trans. Metall. Soc. AIME*, Vol 224 (No. 10), 1962, p 1047-1061
116. D. Kuhlmann-Wilsdorf, Unified Theory of State II and III of Workhardening in Pure FCC Metal Crystals, *Workhardening*, J.P. Hirth and J. Weertman, Ed., Gordon and Breach Science Publishers, 1968, p 97-132
117. D. Kuhlmann-Wilsdorf, Recent Process in Understanding of Pure Metal and Alloy Hardening, *Work Hardening in Tension and Fatigue*, A.W. Thompson, Ed., AIME, 1977, p 1-43
118. D. Kuhlmann-Wilsdorf, Theory of Plastic Deformation: Properties of Low Energy Dislocation Structures, *Mater Sci. Eng. A*, Vol 113 (No. 7), 1989, p 1-41
119. W.R. Cannon, The Contribution of Grain Boundary Sliding to Axial Strain During Diffusion Creep, *Philos. Mag.*, Vol 25 (No. 6), 1972, p 1489-1497
120. I.M. Lifshitz, On the Theory of Diffusion-Viscous Flow of Polycrystalline Bodies, *Sov. Phys. JETP*, Vol 17 (No. 4), p 909-920
121. W.A. Rachinger, Relative Grain Translation in the Plastic Flow of Aluminium, *J. Inst. Met.*, Vol 81 (No. 1), 1952/1953, p 33-41
122. J. Bardeen and C. Herring, Diffusion in Alloys and the Kirkendall Effect, *Imperfections in Nearly Perfect Crystals*, W. Shockely, J.H. Hollomon, R. Maurer, and F. Seitz, John Wiley & Sons, 1952, p 261-288
123. F.V. Lenel and G.S. Ansell, A Theory of Dispersion Strengthening, *Powder Metallurgy*, W. Leszynski, Ed., Interscience, p 267-307
124. A.H. Clauer and B.A. Wilcox, Structure Sensitive Creep Behavior of Crystalline Solids, *Inelastic Behaviour of Solids*, M.F. Kanninen, W.F. Adler, A.R. Rosenfield, and R.I. Jaffee, Ed., McGraw-Hill, 1970, p 301-325
125. F.A. Mohamed, K.-T. Park, and E.J. Lavernia, Creep Behavior of Discontinuous SiC-Al Composites, *Mater Sci. Eng. A*, Vol 150 (No. 1), 1992, p 21-35
126. P.W. Davies, G. Nelmes, K.R. Williams, and B. Wilshire, Stress-Change Experiments During High-Temperature Creep of Copper, Iron, and Zinc, *Met. Sci. J.*, Vol 7 (No. 5), 1973, p 87-92
127. K.R. Williams and B. Wilshire, On the Stress- and Temperature-Dependence of Creep of Nimonic 80A, *Met. Sci. J.*, Vol 7 (No. 9), 1973, p 176-179

128. J.D. Parker and B. Wilshire, The Effect of a Dispersion of Cobalt Particles on High-Temperature Creep of Copper, *Met. Sci. J.*, Vol 9 (No. 5), 1975, p 248-252
129. S. Purushothaman and J.K. Tien, Role of Back Stress in the Creep Behavior of Particle Strengthened Alloys, *Acta Metall.*, Vol 26 (No. 4), 1978, p 519-528
130. D. Lazarus, Diffusion in Metals, *Solid State Phys.*, Vol 10, 1960, p 71-126
131. P.G. Shewmon, *Diffusion in Solids*, McGraw-Hill, 1963
132. N.L. Peterson, Diffusion in Metals, *Solid State Phys.*, Vol 22, 1968
133. *CRC Handbook of Chemistry and Physics*, 74th ed., D.R. Lide, Ed., CRC Press, 1993-1994
134. G.S. Ansell and J. Weertman, Creep of Dispersion-Hardened Aluminum Alloy, *Trans. AIME*, Vol 215 (No. 10), 1959, p 838-843
135. R. Lagneborg, Recovery Creep in Materials Hardened by a Second Phase, *J. Mater Sci.*, Vol 3 (No. 11), 1968, p 596-602
136. J.L. Strudel, Mechanical Properties of Multiphase Alloys, *Physical Metallurgy*, 3rd ed., R.W. Cahn and P. Haasen, Ed., North Holland Physics, 1983, p 1411-1486
137. W.C. Oliver and W.D. Nix, High Temperature Deformation of Oxide Dispersion Strengthened Al and Al-Mg Solid Solutions, *Acta Metall.*, Vol 30 (No. 7), 1982, p 1335-1347
138. E. Orowan, Dislocations and Mechanical Properties, *Dislocations in Metals*, M. Cohn, Ed., AIME, 1954, p 69
139. U.F. Kocks, A Statistical Theory of Flow Stress and Work-Hardening, *Philos. Mag.*, Vol 13 (No. 123), 1966, p 541-566
140. R.S.W. Shewfelt and L.M. Brown, High-Temperature Strength of Dispersion-Hardened Single Crystals, II. Theory, *Philos. Mag.*, Vol 35 (No. 4), 1977, p 945-962
141. E. Arzt and M.F. Ashby, Threshold Stresses in Materials Containing Dispersed Particles, *Scr Metall.*, Vol 16 (No. 11), 1982, p 1285-1290
142. E. Arzt and D.S. Wilkinson, Threshold Stresses for Dislocation Climb Over Hard Particles: The Effect of an Attractive Interaction, *Acta Metall.*, Vol 34 (No. 10), 1986, p 1893-1898
143. E. Arzt and J. Rösler, The Kinetics of Dislocation Climb Over Hard Particles—II. Effects of an Attractive Particle-Dislocation Interaction, *Acta Metall.*, Vol 36 (No. 4), 1988, p 1053-1060
144. J. Rösler and E. Arzt, A New Model-Based Creep Equation for Dispersion Strengthened Materials, *Acta Metall. Mater*, Vol 38 (No. 4), 1990, p 671-683
145. A. Orlová and J. Cadek, On Rösler and Arzt's New Model of Creep in Dispersion Strengthened Alloys, *Acta Metall. Mater*, Vol 40 (No. 8), 1992, p 1865-1871
146. G.M. Pharr and W.D. Nix, A Comparison of the Orowan Stress with the Threshold Stress for Creep for Ni-20Cr-2ThO_2 Single Crystals, *Scr Metall.*, Vol 10 (No. 11), 1976, p 1007-1010
147. R. Lagneborg, Bypassing of Dislocations Past Particles by a Climb Mechanism, *Scr Metall.*, Vol 7 (No. 6), 1973, p 605-614
148. W. Blum and B. Reppich, Creep of Particle-Strengthened Alloys, *Creep Behaviour of Crystalline Solids*, B. Wilshire and R.W. Evans, Ed., Pineridge Press, 1985, p 83-135
149. J.H. Hausselt and W.D. Nix, A Model for High Temperature Deformation of Dispersion Strengthened Metals Based on Substructural Observations in Ni-20Cr-2ThO_2, *Acta Metall.*, Vol 25 (No. 12), 1977, p 1491-1502
150. D.J. Srolovitz, R.A. Petkovic-Luton, and M.J. Luton, Edge Dislocation-Circular Inclusion Interactions at Elevated Temperatures, *Acta Metall.*, Vol 31 (No. 12), 1983, p 2151-2159
151. D.R. Srolovitz, M.J. Luton, R. Petkovic-Luton, D.M. Barnett, and W.D. Nix, Diffusionally Modified Dislocation-Particle Elastic Interactions, *Acta Metall.*, Vol 32 (No. 7), 1984, p 1079-1088
152. V.C. Nardone and J.K. Tien, Pinning of Dislocation on the Departure Side of Strengthening Dispersoids, *Scr Metall.*, Vol 17 (No. 4), 1983, p 467-470
153. J.H. Schröder and E. Arzt, Weak Beam Studies of Dislocation/Dispersoid Interaction in an ODS Superalloy, *Scr Metall.*, Vol 19 (No. 9), 1985, p 1129-1134
154. R.S. Herrik, J.R. Weertman, R. Petkovic-Luton, and M.J. Luton, Dislocation/Particle Interactions in an Oxide Dispersion Strengthened Alloy, *Scr Metall.*, Vol 22 (No. 12), 1988, p 1879-1884
155. A. Orlová, K. Kucharová, J. Brezina, J. Krejcí, and J. Cadek, High Temperature Creep in an Al_4C_3 Dispersion Strengthened Aluminium Alloy in Tension and Compression, *Scr Metall. Mater*, Vol 29 (No. 1), 1993, p 63-68
156. G. Schoek, *Dislocations in Solids*, Vol 3, F.R.N. Nabarro, Ed., North-Holland Physics, 1980, p.63-163
157. S.T. Mileiko, Steady State Creep of a Composite Material with Short Fibres, *J. Mater Sci.*, Vol 5 (No. 3), 1970, p 254-261
158. D. McLean, Viscous Flow of Aligned Composites, *J. Mater Sci.*, Vol 7 (No. 1), 1972, p 98-104
159. A. Kelly and K.N. Street, Creep of Discontinuous Fibre Composites, I. Experimental Behaviour of Lead-Phosphor Bronze, *Proc. R. Soc. (London) A*, Vol 328 (No. 1573), 1972, p 267-282
160. A. Kelly and K.N. Street, Creep of Discontinuous Fibre Composites, II. Theory for the Steady-State, *Proc. R. Soc. (London) A*, Vol 328 (No. 1573), 1972, p 283-293
161. H. Lilholt, Relations Between Matrix and Composite Creep Behaviour, *Proc. Risφ Int. Symp. on Metallurgy and Materials Science, 3rd (Fatigue and Creep of Composites Materials)*, H. Lilholt and R. Talreja, Ed., Risφ National Laboratory, 1982, p 63-76
162. V.C. Nardone and K.M. Prewo, On the Strength of Discontinuous Silicon Carbide Reinforced Aluminum Composites, *Scr Metall.*, Vol 20 (No. 1), 1986, p 43-48
163. M. Taya and H. Lilholt, Modeling of the Second and Third Stage Creep Rates of Aligned Short Fiber Metal Matrix Composites, *Advances in Composite Materials and Structures*, S.S. Wang and Y. Rajapakse, Ed., ASME, 1986, p 21-27
164. T. Morimoto, T. Yamaoko, H. Lilholt, and M. Taya, Second Stage Creep of SiC Whisker/6061 Aluminum Composite at 573 K, *J. Eng. Mater Tech. (Trans. ASME, Series H)*, Vol 110 (No. 2), 1988, p 70-76
165. T.L. Dragone and W.D. Nix, Geometric Factors Affecting the Internal Stress Distribution and High Temperature Creep Rate of Discontinuous Fiber Reinforced Metals, *Acta Metall. Mater*, Vol 38 (No. 10), 1990, p 1941-1953
166. M. Tanaka, Prediction of Creep Deformation in Ductile Two-Phase Alloys by a Continuum Mechanics Model, *J. Mater Sci.*, Vol 28 (No. 10), 1993, p 2750-2756
167. G. González-Doncel and O.D. Sherby, High Temperature Creep Behavior of Metal Matrix Aluminum-SiC Composites, *Acta Metall. Mater*, Vol 41 (No. 10), 1993, p 2797-2805
168. S. Purushothaman and J.K. Tien, Role of Back Stress in the Creep Behavior of Particle Strengthened Alloys, *Acta Metall.*, Vol 26 (No. 4), 1978, p 519-528
169. S. Purushothaman, O. Ajaja, and J.K. Tien, On the Concept of Back Stress in Particle Strengthened Alloys, *Strength of Metals and Alloys*, Vol 1, P. Haasen, V. Gerold, and G. Kostorz, Ed., Pergamon, 1979, p 251-257
170. O. Ajaja, T.E. Howson, S. Purushothaman, and J.K. Tien, The Role of the Alloy Matrix in the Creep Behavior of Particle-Strengthened Alloys, *Mater Sci. Eng.*, Vol 44 (No. 2), 1980, p 165-172
171. J.S. Benjamin, Dispersion Strengthened Superalloys by Mechanical and Alloying, *Metall. Trans.*, Vol 1 (No. 10), 1970, p 2943-2951
172. J.S. Benjamin and M.J. Bomford, Dispersion Strengthened Aluminum Made by Mechanical Alloying, *Metall. Trans. A*, Vol 8 (No. 8), 1977, p 1301-1305
173. P.S. Gilman and J.S. Benjamin, Mechanical Alloying, *Ann. Rev. Mater Sci.*, Vol 13, 1983, p 279-300

174. N.S. Stoloff, Fundamentals of Strengthening, *The Superalloys*, C.T. Sims and W.C. Hagel, Ed., Wiley, 1972, p 79-111
175. P. Haasen, Mechanical Properties of Solid Solutions, *Fundamental Aspects of Structural Alloy Design*, R.I. Jaffee and B.A. Wilcox, Ed., Plenum Publishing, 1975, p 3-25
176. *Alloy and Structural Design*, J.K. Tien and G.S. Ansell, Ed., Academic Press, 1976
177. L. Shi, J. Chen, and D.O. Northwood, Inclusion Control in a 16Mn Steel Using a Combined Rare Earth and Calcium Treatment, *J. Mater Eng.*, Vol 13 (No. 4), 1991, p 273-279
178. L. Shi, J. Chen, and D.O. Northwood, Effect of Rare Earth and Calcium Treatments on the Mechanical, Physical, and Electrochemical Properties of a 16Mn Steel, *J. Mater Eng. Perform.*, Vol 1 (No. 1), 1992, p 21-28
179. L. Shi and D.O. Northwood, Effect of Rare-Earth and Calcium Treatment on the Banded Microstructure and Fracture Properties of a 16 Mn Steel, *J. Mater Sci.*, Vol 27 (No. 19), 1992, p 5343-5347
180. L. Shi, D.O. Northwood, and Z. Cao, Alloy Design and Microstructure of a Biomedical Co-Cr Alloy, *J. Mater Sci.*, Vol 28 (No. 5), 1993, p 1312-1316
181. L. Shi, D.O. Northwood, and Z. Cao, The Properties of a Wrought Biomedical Cobalt-Chromium Alloy, *J. Mater Sci.*, Vol 29 (No. 5), 1994, p 1233-1238
182. *Intermetallic Compounds*, J.H. Westbrook, Ed., John Wiley & Sons, 1967
183. *Alloying*, J.L. Walter, M.R. Jackson, and C.T. Sims, Ed., American Society for Metals, 1980
184. R. Raj and M.F. Ashby, On Grain Boundary Sliding and Diffusional Creep, *Metall. Trans.*, Vol 2 (No. 4), 1971, p 1113-1127
185. M.F. Ashby and R.A. Verrall, Diffusion-Accommodated Flow and Superplasticity, *Acta Metall.*, Vol 21 (No. 2), 1973, p 149-163
186. R.C. Gifkins, Grain-Boundary Sliding and Its Accommodation During Creep and Superplasticity, *Metall. Trans. A*, Vol 7 (No. 8), 1976, p 1225-1232
187. A.K. Ghosh and R. Raj, Grain Size Distribution Effects in Superplasticity, *Acta Metall.*, Vol 29 (No. 4), 1981, p 607-616
188. R. Raj, Creep in Polycrystalline Aggregates by Matter Transport Through a Liquid Phase, *J. Geophys. Res.*, Vol 87 (No. B6), 1982, p 4731-4739
189. G.M. Pharr and M.F. Ashby, On Creep Enhanced by a Liquid Phase, *Acta Metall.*, Vol 31 (No. 1), 1983, p 129-138
190. D.R. Clarke, High-Temperature Deformation of a Polycrystalline Alumina Containing an Intergranular Glass Phase, *J. Mater Sci.*, Vol 20 (No. 4), 1985, p 1321-1332
191. B.L. Vaandrager and G.M. Pharr, Compressive Creep of Copper Containing a Liquid Bismuth Intergranular Phase, *Acta Metall.*, Vol 37 (No. 4), 1989, p 1057-1066
192. J.R. Dryden, D. Kucerovsky, D.S. Wilkinson, and D.F. Watt, Creep Deformation Due to a Viscous Grain Boundary Phase, *Acta Metall.*, Vol 37 (No. 7), 1989, p 2007-2015
193. R.C. Gifkins, Factors Influencing Deformation of Superplastic Alloys. Part I: Grain-Size Distribution, *Mater Forum*, Vol 13 (No. 4), 1989, p 279-287
194. R.C. Gifkins, Factors Influencing Deformation of Superplastic Alloys. Part II: Grain-Size Boundary Sliding, *Mater Forum*, Vol 15 (No. 1), 1991, p 82-94
195. L. Shi and D.O. Northwood, A "Phase" Approach to Superplastic Deformation, *Acta Metall. Mater*, Vol 40 (No. 8), 1992, p 2069-2074
196. M.M. Chadwick, D.S. Wilkinson, and J.R. Dryden, Creep Due to a Non-Newtonian Grain Boundary Phase, *J. Am. Ceram. Soc.*, Vol 75 (No. 9), 1992, p 2327-2334
197. M.M. Chadwick, R.S. Jupp, and D.S. Wilkinson, Creep Behavior of a Sintered Silicon Nitride, *J. Am. Ceram. Soc.*, Vol 76 (No. 2), 1993, p 385-396
198. J.W. Martin, Micromechanisms at Elevated Temperatures, *Micromechanisms in Particle-Hardened Alloys*, Cambridge University Press, 1980, p 151-192
199. H.E. Evans, *Mechanisms of Creep Fracture*, Elsevier, 1984
200. H.G.F. Wilsdorf, Dispersion Strengthening of Aluminum Alloys, *Dispersion Strengthened Aluminum Alloys*, Y.-W. Kim and W. Griffith, Ed., TMS, 1988, p 3-29
201. J.A. Hawk, P.K. Mirchandani, R.C. Benn, and H.G.F. Wilsdorf, Evaluation of the Elevated Temperature Strength and Microstructural Stability of Dispersion Strengthened MA Aluminum Alloys, *Dispersion Strengthened Aluminum Alloys*, Y.-W. Kim and W. Griffith, Ed., TMS, 1988, p 517-537
202. H.G.F. Wilsdorf and D. Kuhlmann-Wilsdorf, Work Softening and Hall-Petch Hardening in Extruded Mechanically Alloyed Alloys, *Mater Sci. Eng. A*, Vol 164 (No. 1/2), 1993, p 1-14
203. W. Schneider and H. Mughrabi, Investigation of the Creep and Rupture Behaviour of the Single-Crystal Nickel-Base Superalloy CMSX-4 Between 800 °C and 1100 °C, *Proc. of 5th Int. Conf. on Creep and Fracture of Engineering Materials and Structures*, B. Wilshire and R.W. Evans, Ed., The Inst. of Materials, 1993, p 209-220
204. T. Yokokawa, K. Ohno, H. Harada, S. Nakazawa, T. Yamagata, and M. Yamazaki, Towards an Intelligent Computer Program for the Design of Ni-Base Superalloys, *Proc. of 5th Int. Conf. on Creep and Fracture of Engineering Materials and Structures*, B. Wilshire and R.W. Evans, Ed., The Inst. of Materials, 1993, p 245-254
205. H. Harada, T. Yamagata, T. Yokokawa, K. Ohno, and M. Yamazaki, Computer Analysis on Microstructure and Property of Nickel-Base Single Crystal Superalloys, *Proc. of 5th Int. Conf. on Creep and Fracture of Engineering Materials and Structures*, B. Wilshire and R.W. Evans, Ed., The Inst. of Materials, 1993, p 255-264